Dissertations, Theses, and Masters Projects   Theses, Dissertations, & Master Projects

2015

A Mathematical Model of Tau Protein Hyperphosphorylation: The Effects of Kinase Inhibitors as a Theoretical Alzheimer's Disease Therapy

Patrick Neil Blank
College of William & Mary - Arts & Sciences

A Mathematical Model of Tau Protein Hyperphosphorylation
The Effects of Kinase Inhibitors as a Theoretical Alzheimer's Disease Therapy

Patrick Neil Blank .

Richmond, Virginia

BS, The College of William and Mary, 2013

A Thesis Presented to the Graduate Faculty
of The College of William and Mary in Candidacy for the Degree of
Master of Science

Department of Chemistry

The College of William and Mary
August, 2015

APPROVAL PAGE

This Thesis is Submitted in Partial Fulfillment of
the Requirements for the Degree of

Master of Science

_____
Patrick Neil Blank

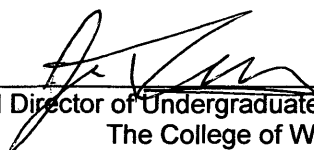Approved by the Committee, May 8th, 2015

_____
Committee Chair
Associate Professor Randolph A. Coleman, Chemistry
The College of William and Mary

_____
Chancellor Professor and Department Chair Christopher J. Abelt, Chemistry
The College of William and Mary

_____
Professor and Director of Undergraduate Studies John C. Poutsma, Chemistry
The College of William and Mary

ABSTRACT

Using Biological Systems Theory (BST), our group builds intricate computer models of neurodegenerative diseases and associated processes to simulate the activities occurring within the cell regarding the disease of interest, utilizing CellDesigner 4.3 and MATLAB R2014a. This particular project primarily models Tau protein, as it is one of the most implicated proteins in Alzheimer's disease. Intraneuronal hyperphosphorylated Tau protein leads to neurofibrillary tangles, which cause apoptosis. The model eventually resulted in the generation of optimal drug concentrations for molecules used theoretically as Tau protein kinase inhibitors, ultimately allowing the isolation of SP-600125 as the best mathematical solution to the biochemical problem presented in the form of our system of differential equations comprising aforementioned model. SP-600125 was determined as the best, but many other drugs performed well in this theoretical simulation of disease therapy.

TABLE OF CONTENTS

ACKNOWLEDGEMENTS

This thesis is dedicated to my best friend, Matthew 'Harvard' Weber, for always pushing
me to persevere and strive for excellence not only in academics, but in life itself …

LIST OF FIGURES

HISTORY

Dementia seems to have been plaguing mankind since Ancient Greece through the modern era, its most extreme case discovered and thence classified by Alois Alzheimer as Alzheimer's disease in 1906 (AD 2013). Karl Deter, a man of Frankfurt, Germany brought his wife, Auguste Deter, to a hospital for the mentally ill in 1901, where she was brought immediately to the director of said hospital, Alois Alzheimer. A psychiatrist and neuropathologist, Dr. Alzheimer was quick to note in Auguste's patient file that she was very advanced in her dementia (AD 2013), especially noting her sense of overwhelming helplessness and inability to write despite her being a literate, 50 year old. Five years later, she passed away after experiencing severely worsened symptoms including but not limited to illusions and hallucinations; Alzheimer and others were quick to examine her brain. His specific findings would lead to discovery of neurofibrillary tangles, the main biological association with the disease (AD 2013). Despite this association, there is currently no known cure . .

INTRODUCTION AND BACKGROUND

The nervous system is what allows the human body to complete both voluntary and involuntary actions via the transmission of electric signals. The brain is part of the central nervous system, or CNS. The human brain is commonly thought of as having three main parts: the forebrain, midbrain, and hindbrain generally responsible for complex thought processing, reflexes, and vital body functions respectively. The cerebrum is also referred to as the cortex which is the outermost portion of the brain, consisting of the frontal, parietal, occipital, and temporal lobes. The cerebrum, thalamus, and hypothalamus comprise the forebrain; the tectum and tegmentum comprise the midbrain; and the cerebellum, pons, and medulla comprise the hindbrain. The thalamus and hypothalamus are part of what is referred to as the limbic system, along with the amygdala and most importantly, the hippocampus. The hippocampus resides within the medial temporal lobe and is associated with memory, and it is for this reason that the cells of this brain component are heavily investigated by scientists researching memory loss. Alzheimer's disease researchers make particularly heavy use of hippocampal cell lines, but that is not to say that these are the only types of cells affected by the disease.

A grey matter type brain cell called a neuron has a cell body has a nucleus with expected organelles such as a golgi apparatus, ribosomes, and mitochondria. This cell

2

body in turn receives information from other neurons chemically via attached branching formations called dendrites. Dendrites, at specific points, are covered in receptors which receive information in the form of neurotransmitters released from neighboring neuron axonal synapses. Throughout the dendrites and axons alike are microfilaments and microtubules which maintain the cell's structural integrity, just like that of any eukaryotic cell. Microtubules play the largest cytoskeletal role here, and are kept together mainly by microtubule-associated proteins, or MAPs. One of the most important types of MAPs are the Tau variety, which play a major factor in promoting tubulin assembly into the microtubule morphology (Koralova 2). However, in the neurons of people diagnosed with Alzheimer's disease, tau proteins form aggregates and develop an inability to bind tubulin through the normal phosphorylation-regulated method. The microtubules literally fall apart without the integration of tau protein stabilizing them, resulting in neurodegeneration and cell death, which causes memory loss primarily.

Tau Protein

Tau proteins are particularly large, ranging in molecular weight between 55,000 and 62,000 grams per mole. They are rod-like in overall structure, and are tens of nanometers in length on average. This length and size proves crucial in the binding of microtubules, especially in the rod-like shape of a neuronal axon (Hirokawa 1449). Tau proteins tend to act like short cross bridges, integrating themselves throughout the microtubule via disseminated binding to the point where the microtubule ascertains a

slightly higher elasticity. This elasticity allows cross linking of microtubules, which provides healthy neurons with augmented structural integrity (Hirokawa 1451).

Tau is not the only important MAP, but is most interesting because it seems to have a large number of inherent properties, such as the fact that it is a natively unfolded protein (Koralova 2). This means that it can undergo many transformations or modifications which result in varying degrees of conformations. Researchers are actively trying to discover which relationship, whether it be phosphorylation, proteolysis, oxidation or glycosylation, is an active cause of the neurofibrillary build up as seen in AD patients.

Tau has many phosphorylation sites on its unfolded native structure, meaning that hyper-phosphorylation, when more phosphate groups bind than the substrate molecule requires to perform a specific function, certainly can occur (Mandelkow 8). Phosphorylation of Tau usually results in 2 phosphate groups per Tau molecule in healthy neurons, but AD diseased neurons typically show upwards of 8. However, it has been shown that this hyper-phosphorylation is not uncommon in fetal neurons nor in animals whom undergo hibernation, marking it by many as mere coincidence. This has been supported by similar levels of phosphatase and other enzymes who catalyze phosphorylation in hyper-phosphorylated cellular environments (Mandelkow 9). However, it has also been shown that the hyper-phosphorylation of Tau proteins weakens their affinity to microtubules, thus increasing the probability that Tau aggregations will form with an increased number of Tau – Tau collisions occurring due to free Tau protein inside the cell. It is clear that both stances on Tau phosphorylation still need further study (Mandelkow 9).

In addition to phosphorylation, Tau proteins often undergo proteolytic

cleavage, which is the breakdown of a protein into its consisting peptides and

sometimes to the extent of amino acid monomers. Proteases easily access the unfolded

Tau and essentially cleave it into its smaller pieces (Mandelkow 10). Sometimes,

however, it does not get entirely broken down; cysteine-aspartic proteases for example

cleave only the Tau tails, which in turn prevent its folding into conformations proven

less prone to aggregation. There are numerous examples of proteases, like this one,

that are aggregation stimulating in nature, but there are those which clip the Tau into

potential configurations which have propensities to conform structures which oppose

Tau-Tau interlinking and therefore aggregation. The key here is to inhibit the

aggregation stimulating protease functions and stimulate the aggregation inhibiting

protease functions, which is easier said than done (Mandelkow 10).

Tau proteins can also undergo oxidation. This occurs at the cysteine-322

region of paired Tau helical filaments. Oxidation here allows for disulfide bridging to

more easily occur and dimer cross links to form (Mandelkow 10), heightening

aggregation propensity as well as essentially locking already aggregated Tau proteins,

two results which are respectively negatively impactful on diseased neurons.

Finally, the last primary transformation undergone by many Tau proteins is

glycosylation. Glycosylation, being the process by which a carbohydrate is attached to

a hydroxyl or other functional substituent of a molecule, is normally a very good thing

for Tau proteins because it protects against hyper-phosphorylation (Mandelkow 10). If

the open sites to phosphorylation are not directly bound by carbohydrates through this

process, steric interactions between bound carbohydrate chains and incoming

5

phosphates may be what decreases the likelihood of phosphate binding. However, in AD diseased neurons, glycosylated Tau proteins become defective regarding phosphorylation, stimulating binding and thus increasing the propensity for hyper-phosphorylation (Mandelkow 10). The reason for these defectives arising is a currently researched, unsolved mystery.

Since Alois Alzheimer's time, it has proven difficult to identify causes or at least correlations between factors such as Tau proteins and Alzheimer's disease. The results appear to be sporadic, in that there is a lack of compelling evidence pointing toward genetic involvement, as 1-5% of all diagnosed have been deemed so based on heredity. It seems the best way to identify the disease in general, and thereby have a longer period to discover causes before death ensues, is through the seven stage process endorsed by the Alzheimer's Association.

Seven Stages of Alzheimer's Disease

The first stage is that of a normal functioning human being who has zero impairment whatsoever despite uncommon absentmindedness or even forgetfulness due to stress and other day to day factors. As previously described, someone experiencing said minor mishaps would not be diagnosed with dementia by a medical professional, but perhaps something more along the lines of issues regarding the ability to focus, pay attention, et cetera.

Stage two goes beyond the uncommon mental mishap to envelop the occurrences which involve important things such as the names of familiar objects and commonly used words of the pertinent language. These are described as memory

lapses and are often noticed by the victim of said lapses. Instances such as these would still be unclassified as dementia by medical professionals, and usually not noticed by relatives or persons of everyday contact.

Stage three is that of mild cognitive decline in which names are difficult to recall of newly introduced persons, particularly valuable objects are lost in the same proportion to those considered invaluable, and difficulty performing assigned tasks. Often mild cognitive decline results in memory loss of things that have just been read or seen and has also been associated with increasing difficulty regarding organizational skills and planning. Medical professionals would be able to diagnose some mild cognitive declining persons with early onset Alzehimer's disease, but not all; some may be alternatively diagnosed with issues pertaining to concentration.

Stage four pertains to those persons with moderate cognitive decline. Symptoms here include forgetfulness of recent events, inability to perform challenging mental arithmetic, more difficulty than mild cognitive declining persons regarding planning or social management, and most importantly, forgetting facts about one's own personal history. Previously, stages one through three involved potential forgetfulness regarding others or even surroundings, but stage 4 is clearly identified by rare forgetfulness of topics that a person should always know about themselves. Medical professionals would diagnose a stage four person with either early-onset or mild Alzheimer's disease based on the compilation of symptoms.

Stage five pertains to those persons with moderately severe cognitive decline, meaning that they have very externally noticeable gaps in memory and thinking ability. Symptoms include but are not limited to recalling a personal address or phone

number, knowledge of the day's date, inability to perform non-challenging mental arithmetic, and inability to choose clothing pertinent to the weather. Discerning stage five and beyond becomes increasingly difficult, so it is common to note things that persons in these stages are still able to do: stage five persons still remember personal topics, however less so than stage four, and are still able to go to the bathroom unassisted. Medical professionals would now be able to diagnose these persons with moderate or mid-stage Alzheimer's disease.

Stage six pertains to those persons severe cognitive decline. The experiences and symptoms that may be pertinent include forgetting where one is or one's surroundings, strange personality changes, needing help getting dressed entirely, changes in sleep patterns, delusional behavior, and frequent loss of bowel control. However, stage six is most often identified by ability to still remember one's own name, despite loss of almost all personal history recollection. Medical professionals could diagnose a stage six person with moderately severe Alzheimer's disease.

The final stage is stage seven. Stage seven is the worst step of the disease, as those afflicted experience very severe cognitive decline. Basically, in this stage, all ability to establish a long term connection with their environment is lost. Some spurts of memory recollection have been noted, but are also all accompanied by another note saying that the same memory recollection happens often. Further, a very well off stage seven person may have an intriguing introduction and conversation with a healthy person, but then immediately forget the events which may have taken place seconds ago and attempt to re-introduce his or herself as if nothing ever happened. This is the best circumstance, whereas the worst off stage seven persons cannot cloth, feed, nor

clean themselves without assistance; many of the symptoms associated with Alzheimer's disease are associated with those of an infant. This is not a coincidence, as things such as daily hygiene are learned and upon stage seven onset of AD, are fully unlearned and essentially destroyed cognitions.

In addition to severe social symptoms, severe physical symptoms are experienced by stage seven persons as well which delve beyond those experienced in infanthood, including loss or at least impaired motor control. For example, many lose the ability to swallow food, something that is done regularly and naturally by infants, despite their still relying on being fed in the first place. Others lose the ability to react with reflexes, smile, and even keep a straight neck before ultimately losing all cognitive abilities and dying thenceforth.

Amyloid Beta Peptide

One of the most implicated molecules in AD neurodegeneration is the amyloid-beta (Aβ) peptide. Aβ is hydrophobic and can have a primary protein structure over 40 amino acids long. It is the proteolytic result of Amyloid Precursor Protein (APP) cleavage by proteases such as β-secretase (Lichtenthaler 10). Currently, it is known that there are two major competing AD secretase pathways: the α-secretase pathway and the β-secretase pathway. The minor pathway is of the γ variety, appropriately known as the γ-secretase pathway. These pathways constitute what are ʿ called the non-amyloidogenic and the amyloidogenic pathways.

The non-amyloidogenic pathway is responsible for 90% of the APP cleavage activity, and is the pathway which does not lead to the generation of Aβ. This pathway

involves the metalloprotease α-secretase cleaving APP to yield the shedding of a soluble APP fragment (sAPPα), leaving behind a carboxy terminal fragment (CTF) composed of 83 amino acids with a C-terminus (C83). This α-secretase cleavage is followed by γ-secretase cleavage of C83, resulting in a peptide fragment (p3) and another fragment referred to as the intracellular domain (AICD). These two resultant fragments are not known to lead to Aβ generation in any way, so the stimulation of α-secretase activity is thought of as being highly therapeutic (Lichtenthaler 11).

The amyloidogenic pathway, correspondingly, is responsible for 10% of the APP cleavage activity, and is the pathway which does in fact lead to the generation of Aβ. This pathway instead involves β-secretase cleaving APP to yield the shedding of sAPPβ and C99. Afterwards, γ-secretase cleaves C99 in the same fashion as C83, but now yields AICD and Aβ. Upon secretion, soluble Aβ is not as neurotoxic as the oligomers which result from Aβ misfolding. These soluble, small oligomers are associated with inflammation, inhibition of hippocampal long term potentiation, synaptic dysfunction, neuronal loss, and especially the formation of neurofibrillary tangles (Lichtenthaler 10). Protofibrils are precursors to these tangles, which lead to neuronal cell death either directly by forming fibrils or indirectly through pathogenic amyloid pores (PAP), which lead to reactive oxygen radical species (ROS). These resulting high energy oxygen radicals are capable of directly causing aforementioned neuronal cell death or indirectly causing it via activation of kinases involved with Tau protein activity.

Roles of the Endosomal System

One organelle that has not been portrayed as much in the Alzheimer's literature is the lysosome. The lysosome is primarily responsible for cellular waste removal in addition to cellular digestion of lingering, unwanted chemical compounds. It acts via hydrolytic enzyme secretion at a low, acidic pH that is enclosed via its membrane. This membrane can fuse with other organelles and endosome systems to engulf the biochemical matter of interest, which can range from foreign microbes to random particles or molecular debris.

The lysosomes of a neuron play a particularly important role in that they comprise what are known as the endocytic and autophagic pathways. These pathways make synaptic transmission of chemical signals and neurotransmitters as well as the degradation of excess organic materials possible. Acceleration of endocytosis essentially can overwhelm the lysosome and cause it to function improperly. This acceleration is caused by APP gene duplication that is a result of CTF accumulation and is mediated by rab5 (Pimplikar 14947). Essentially, efficiency begins to wane and proteolysis effectively halts, resulting in massive debris buildup which visibly swells neurons, changing their optimal conformation. This buildup includes molecules such as $A\beta$, ROS, as well as other toxins that would have otherwise been removed, to an extent, and thence results in neurodegeneration via multiple pathways (Pimplikar 14948). It is clear that this role as well as others makes the lysosome an organelle that should be considered more often when trying to unravel the mysteries of AD neurodegenerative biochemistry. The internalized APP in particular participates in a vicious cycle of amyloidogenesis, generating more and more $A\beta$ via the resultant

11

sequestered fibril environment which has been shown to stimulate the amyloidogenic pathway (Bahr 117).

Aβ can, however, be transported in other ways into the cell. Extracellular Aβ can bind to the α7-nicotinic acetylcholine receptor, or α7nAChR. This receptor is pentameric and is a type of acetylcholine receptor found within the brain, which triggers both presynaptic and postsynaptic excitation. When Aβ binds, it competes competitively resulting in the slowing and even prevention of calcium activation and the release of acetylcholine (Wang 5626). One method used to stop this binding is taking advantage of a chemical called alpha bungarotoxin, or α-BTX.

The α-BTX drug is originally a component of snake venom which causes paralysis and respiratory failure by binding to neuromuscular nicotinic acetylcholine receptors. It has another role that is important in the unraveling AD therapies: its ability to bind α7nAChR in the brain (Nagele 203). The 74 amino acid that is otherwise deadly can be thought of as an alzheimer's therapy in that it can compete with Aβ for binding to α7nAChR. The tricky part is not letting the toxin induce cell death while it prevents Aβ binding, perhaps thwarted by anti-venom.

Upon binding of Aβ to α7nAChR, a complex is formed primarily on neuronal dendrites which can then be transported inside the cell (Nagele 208). In addition to the lysosome, early and late endosomes play an extremely important role in AD neurons because they perform said transportation and thus contribute to the internalization of Aβ. This can be thwarted by phenylarsine oxide, or PAO, which is an endocytosis inhibitor (Nagele 201).

Tau and Aβ are indeed the two most implicated proteins regarding the onset of

Alzheimer's disease. Hyperphosphorylated Tau protein leads to the formation of

intraneuronal neurofibrillary tangles, which destabilize microtubules and result

inevitably in apoptosis. Aβ leads to the formation of dimers, protofibrils, and fibrils

which form interneuronal senile plaques, disruption interneuronal communication and

ultimately inducing apoptosis as well. These two very important intraneuronal and

interneuronal pathways respectively are separated by the cell membrane, but

ultimately connected by intracellular Aβ that has been internalized via methods

described above. This connection arises and is founded on the fact that Aβ stimulates

casein kinase I and casein kinase II (Chauhan 50). These two enzymes are called

kinases because they perform phosphorylation, specifically here on tau protein. The

main focus of my research project thus far has been to study and unravel the

relationships between such kinases and tau apoptosis by mathematically portraying the

best way to lessen apoptosis both intraneuronally and interneuronally. Before I talk

about the methods, I would like to go give an in depth review of the metals, kinases,

drugs, and other molecules involved.

Roles of Metals

Let us not only look at the effects of peptides and organelles on AD, but also at

the role metals play in AD. I started with calcium and learned that it had significant

activity in aiding protein phosphatase 2A with dephosphorylating the

hyperphosphorylated tau proteins characteristic in AD brains. I found it interesting

that calcium being one of the most readily accessible metals in the body through

parathyroid hormone activity on bone cannot simply treat AD in this manner. Aware of the new 'cocktail' approach where it is thought that no one molecule or drug can effectively cure a neurodegenerative disease, I knew there must be another type of metal involved.

Zinc is a 3d transition metal that is an essential mineral to the human body. Zinc deficiency is more common than that of other metals because the human body lacks a specialized zinc storage system. Zinc has important roles in growth and the immune system, but is also an important player when it comes to AD. Zinc has been found to catalyze the conversion of active PP2A to inactive PP2A, as well as directly catalyze the hyperphosphorylation of Tau proteins (Xiong 746). Thus, zinc seems to be in competition with calcium, as they have antonymic effects on Tau proteins. However, remembering that it is an essential mineral because of its other functions throughout the body, zinc is not to be eliminated from the diet as a potential therapeutic treatment. Instead, zinc intake by those with AD should be minimized to the lower end of recommended daily dietary allowance (RDA) range, here being about 9 mg/day. This combined with other treatments could aid and indeed prove therapeutic for those with AD, based on these recent zinc findings.

Lithium is the third element of the periodic table and is the lightest metal in existence. It also is extremely reactive and flammable. It has a wide variety of inorganic applications, ranging from its incorporation into thermonuclear weapon fuel as lithium-6 deuteride to a source of electrons in galvanic cell batteries. There are some bioorganic and medicinal applications as well, including its use in the treatment of mood disorders due to its involvement in the central nervous system as a cation

(Li$^+$). In the brain, however, lithium has been shown to directly inhibit the beta

isoform of Glycogen synthase kinase – 3 Beta (GSK-3β) by competing with

magnesium (Gong 2323). As a result, a relative increase in lithium could prove

therapeutic in AD brains.

Roles of Tau Protein Kinases and Their Respective Activity Modulators

In addition to metals, Alzheimer's disease involves a variety of kinases and

other molecules that can be catalytic regarding the hyperphosphorylation pathway, as

previously mentioned. Pharmacologically, it is much easier and more efficient to

develop drugs with the ability to inhibit these catalysts as opposed to developing drugs

with the ability to activate inhibitors such as aforementioned PPA2. Two of the most

important kinase catalysts in general are cdk-5 and the aforementioned GSK-3β,

which are both proline directed protein kinases, or PDPKs.

GSK-3 is a protein kinase that is associated with adding phosphates to proteins

with threonine and serine primary protein structures, like those found in the tau

protein. This enzyme was discovered and appropriately named in 1980 for its

regulatory involvement regarding glycogen synthase (Embi 519). GSK-3 has an alpha

and a beta form, denoted by GSK-3α and GSK-3β respectively; GSK-3β appears to be

under more scrutiny than the alpha form for its implication in Alzheimer's disease

(Gong 2323). Both forms of GSK-3 share many inhibitors, including Aloisine,

Hymenialdisine, Induribins, and Flavopiridol, and aforementioned Lithium just to

name a few.

An aloisine has a molecular formula of $C_{16}H_{17}N_3O$ and is a potent, permeable

inhibitor of many kinases, including GSK-3 (Gong

2323). They are 6-phenyl[5H]pyrrolo[2,3-b]pyrazines,

as seen in Figure 1, which act in an inhibitory fashion

Figure 1
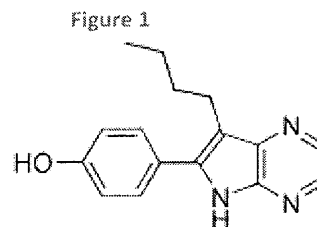
by competitive ATP inhibition; this means that these molecules inhibit the binding of

ATP to the catalytic portion of the kinase (Mettey 222). As a result, a relative increase

in aloisine could prove therapeutic in AD brains.

Among other molecules that are ATP-competitive

inhibitors of GSK-3 are Hymenialdisine and Induribins, which

interestingly enough, are marine- derived. Hymenialdisine,

portrayed by Figure 2, is a natural, marine sponge molecular

Figure 2
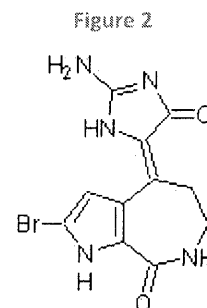
product that has been shown to be inhibitory of GSK-3, among other kinases (Meijer

51). It has three constituent N-heterocyclic rings in its

structure that has many analogues, a few of which are

acetylated or contain bromine substituents (Meijer 51).
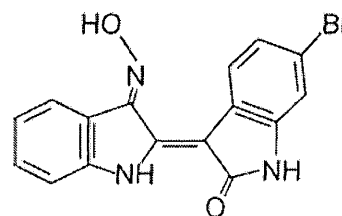
Figure 3

Indirubins are active ingredients in the Danggui Longhui Wan, which is an ancient

Chinese medicinal recipe. These molecules have four rings, as seen in Figure 3, two of

which are N-heterocyclic, and are also inhibitors of GSK-3 as well as other kinases

(Leclerc 251). One induribin in particular is 6-Bromoindirubin-3'-oxime, or 6-BIO.

Crystallography of both hymenialdisine and induribins reveals that these ringed

structures bind nicely to the ATP binding sites of GSK-3, making them prime targets

for AD therapeutic approaches.

16

Flavopiridol, seen in Figure 4 to the right, is a decently large alcohol with four rings, one of which is N-heterocyclic. It has a chlorine 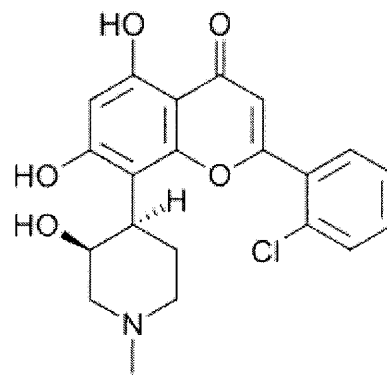substituent as well as a ketone. Its common name is Alvocidib, where it and analogues are used to inhibit kinases other than GSK-3. However, it is

Figure 4

still thought of commonly as a GSK-3 inhibitor as well, proving as an effective treatment for AD and other taupathies (Martinez 377).

AR-014418, seen in Figure 5, is a GSK-3 chemical inhibitor of the beta isoform that has a urea foundation with terminal nitro and methoxybenzyl groups, appropriately called N-(4-Methoxybenzyl)-N'-(5-nitro-1,3-thiazol-2-yl)urea. Its molecular weight is 308.31 g/mol and it has
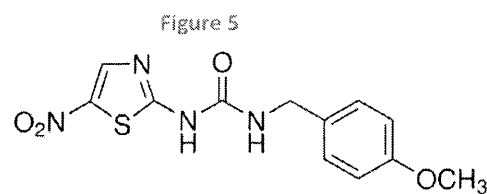

Figure 5

an IC50 value of 104nM on GSK-3 beta. It is also active on CDK-5, but to a much lesser extent, with an IC50 value of over 100 micromolar (Martin 292).

All of these inhibitors to the GSK-3 protein have been found to be therapeutic in targeting tau protein phosphorylation and hyperphosphorylation respectively, but many of these inhibitors and other molecules are also associated with CDK-5, another very important kinase involved in taupathy.

Cyclin-dependent protein kinase 5 (cdk-5) is one of many cyclin-dependent kinases (cdk), but is the most implicated cdk in Alzheimer's disease. This enzyme binds cyclin, a regulatory protein which comes in many varieties ranging from cyclin

17

A – cyclin G, and then becomes able to phosphorylate proteins like Tau. In addition to

aforementioned inhibitors of GSK-3 like Flavopiridol, Aloisine, and Induribins, CDK-

5 has other inhibitors and inhibitor drugs, including Olomoucine, Roscovitine,

Purvalanol, and Paullones. It has activators, some of which are p35 and p39 (Sausville

32).

Cdk-5 cannot function monomerically, for it depends specifically on activators.

These aforementioned activators can each be proteolytically cleaved by calcium

dependent calpains resulting in their smaller forms named p35 and p25, respectively.

The cdk-5/p35 and cdk-5/p25 complexes are much more active than the cdk-5/39 and

cdk-5/29 complexes, contributing moreso thusly to tau protein hyperphosphorylation

(Martin 292).

Olomoucine, or 2-(Hydroxyethylamino)-
6-benzylamino-9-methylpurine, has formula
$C_{15}H_{18}N_6O$ and is a competitive ATP inhibitor of
many cyclin dependent kinases, but CDK-5
especially in the brain. Interestingly, it has also

Figure 6

been shown to regulate CDK-2 in the cell cycle, arresting cleavage in many organisms

(Abraham 105). Olomoucine is portrayed in Figure 6.
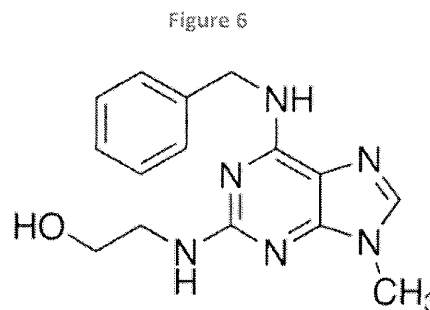
Roscovitine (or Seliciclib), seen in Figure 7, is a
very similar molecule in structure to olomoucine, is
otherwise known as 2-(R)-[[9-(1-Methylethyl)-6-
[(phenylmethyl)amino]-9H-purin-2-yl]amino]-1-
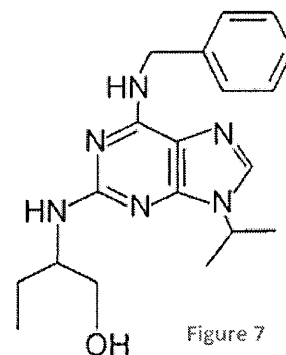butanol, 6-(Benzylamino)-2(R)-[[1-

Figure 7

butanol, 6-(Benzylamino)-2(R)-[[1-

18

(hydroxymethyl)propyl]amino]-9-isopropylpurine with formula $C_{19}H_{26}N_6O$. They can

be easily distinguished by the extra ethyl group off the benzylic nitrogen in

Roscovitine. It is also similar in function to olomoucine, as it inhibits CDK-5

substantially and in a similar manner. Interestingly enough, roscovitine too plays a

role in the cell cycle, proving to be a useful antimitotic reagent (Borgne 527).

Purvalanol differs in structure when
compared generally to olomoucine and roscovitine,
but still maintains the core double N-heterocyclic
ring system. The two forms, Purvalanol A and
Purvalanol B, portrayed by Figures 8 and 9

Figure 8
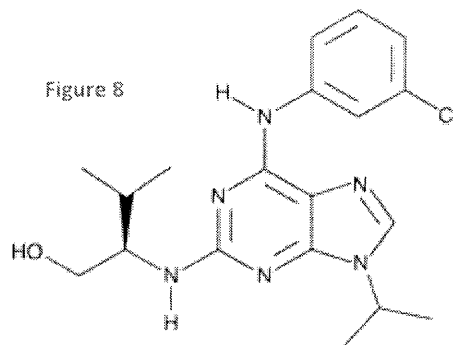
respectively, can be readily distinguished by observing that Purvalanol B has a

benzylic acid group in its chemical structure,
as it is formally named 2-chloro-4-[(2-
{[(2R)- 1-hydroxy-3-methylbutan-2-
yl]amino}-9-(propan-2-yl)-9H-purin-6-
yl)amino]benzoic acid with chemical
formula $C_{20}H_{25}ClN_6O_3$. Purvalanol A,

Figure 9
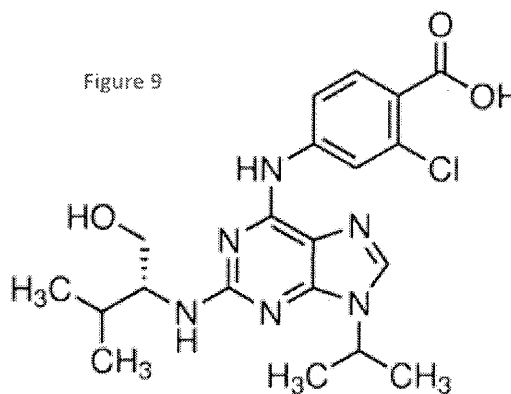
however, just has a chlorine substitutent on that particular benzene group. Purvalanol

in general inhibits many cyclin- dependent kinases (Villerbu 761), and has been used

specifically as a CDK-5 inhibitor. It has been shown to decrease Ser-522 and Thr-

514/409 levels specifically, the residues that have commonly been linked to tau

protein hyperphosphorylation sites (Cole 18230).

Paullones are tetracyclic, fused

compounds that cover a large range of

derivatives with different purposes, many

of which include being inhibitory regarding

cdks and GSK-3 (Martinez 377). They
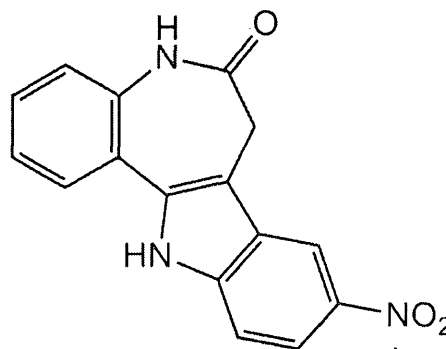
generally are not similar in structure to

Figure 10

olomoucine, roscovitine, nor purvalanol other than the fact that there are still two N-

heterocyclic rings. These two rings are not exactly the same as those found in the other

three molecules due to one of them being 8 membered instead of 6 membered. A

specific type of paullone called alsterpaullone, was shown to be specifically

implicated in the reduction of tau phosphorylation (Selenica 959) and is portrayed

chemically by Figure 10.

R-CR8 , or (2-(R)-(1-ethyl-2-hydroxyethylamino)-6-(4-(2-pyridyl)benzyl)-9-

isopropylpurine) is an interesting

molecule portrayed by Figure 11

which has the exact same structure as

roscovitine in that the only difference

is an extra quinolone substituent
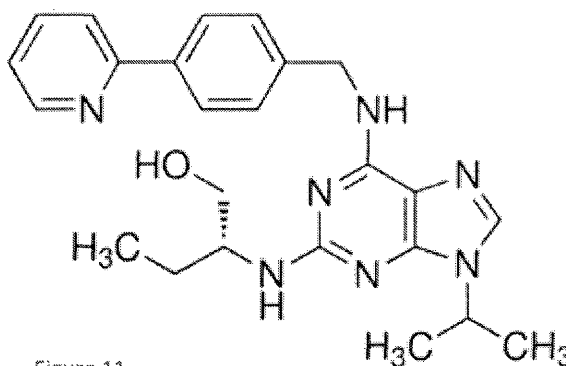
attached to the benzene group. That

Figure 11

being said, it is specifically a derivative of (R)-roscovitine that is thought of as a

versatile inhibitor because it acts on both CDK-5 and GSK-3 (Martin 297).

It seems that generally, a double, fused quinolone N-heterocyclic ring sytem at

the core of a chemical is necessary or at least beneficial to its action as a CDK-5

20

inhibitor, especially for those which are ATP competitive. This structure, or one that is similar, appears in many of the drugs that are being designed for this purpose, and should be maintained in the development of drugs specifically designed for AD therapy to minimize tau protein phosphorylation and hyperphosphorylation.

CDK-5 and GSK-3 may be the most generally well known kinases involved in neurodegenerative diseases, but casein kinases are particularly important in Alzheimer's disease and my research project specifically, as previously mentioned. Casein kinases are non-proline directed protein kinases, or non-PDPK, and have two main types each with its own isoforms.

Casein Kinase 1, or CK1 has 7 different isoforms known as CK1-α, CK1-β, CK1-γ1, CK1-γ2, CK1-γ3, CK1-δ, and CK1-ϵ which range in molecular weight from 25 to 55 kDa. The CK1-α, CK1-δ, and CK1-ϵ isoforms are involved specifically in Alzheimer's disease (Martin 298). These three isoforms are also referred to as CSNK1A1, CSNK1D, and CSNK1E respectively and are known to phosphorylate tau protein.

Casein Kinase 2, or CK2 has three isoforms, CK2-α, CK2-α', and CK2-β. CK2-α and CK2-α' are involved in Alzheimer's disease and are also referred to as CSNK2A1 and CSNK2A2 respectively. Both phosphorylate tau, while each also has an interestingly unique additional function: CK2-α activates PP2A and CK2-α' inhibits PP2A (Martin 298). PP2A is a protein phosphatase, which effectively has a reverse kinase effect on tau protein by removing phosphate.

Both CK1 and CK2 proteins undergo aforementioned activation by Aβ, but are also subject to inhibition by several chemicals including Heparin, TBCA, and IC261 which interestingly differ greatly in structure.

Heparin, seen structurally in Figure 12, is a relatively large molecular weight drug averaging around 13.5 kg/mol that has forever been used in a sulfated form to act as an anticoagulant. However, since the 1980s, Heparin has been shown to be an effective inhibitor of CK2-α and CK2-α' CK-2 variants. (Hathaway 8040).
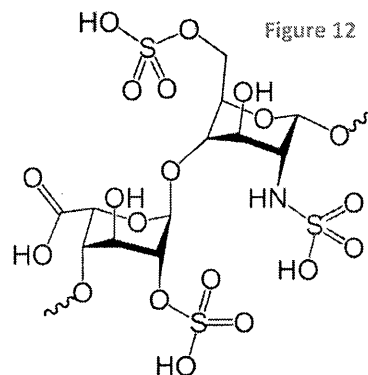
Figure 12

Tetrabromocinnamic acid, or TBCA, is portrayed by Figure 13 and is a small drug compared with the inhibitors acting on GSK-3 and CDK-5, with systematic name (2E)-3-(2,3,4,5-Tetrabromophenyl)acrylic acid. Its main features are the four bromines on the phenyl group which are complemented by the acid group on the other end of the molecule. It is exceptionally more potent of an inhibitor on CK2- α, CK2-α', and CK2-β than on CK1-α, CK1- δ, and CK1-ε, but is regardless an inhibitor of both types of casein kinases (Martin 298).

Figure 13
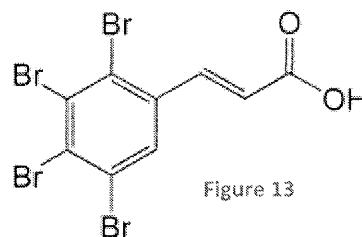
IC261, or 1,3-Dihydro-3-[(2,4,6-trimethoxyphenyl)methylene]-2H-indol-2-one, is a chemical that effectively inhibits CK1-α, CK1- δ, and CK1-ε, but has a particularly potent activity on CK1- δ, with a remarkable IC50 of just 1.0 micromolar (Martin
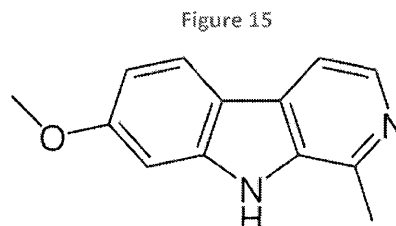
Figure 14
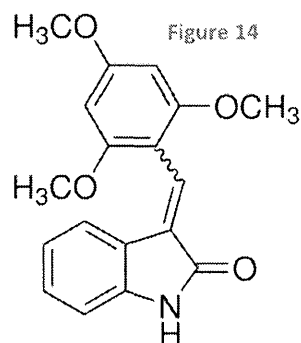
298). It is easily distinguished structurally by its symmetrical trimethoxyphenyl group and has a molecular weight of 311.33 g/mol.

Tau Tubulin Kinase, or TTBK, is another non-proline directed protein kinase that is also known as Brain-Derived Tau Kinase, or BDTK. There are two varieties of TTBK, called Tau Tubulin Kinase-1, or TTBK-1 and Tau Tubulin Kinase-2, or TTBK-2. TTBK-1 and TTBK-2 are very similar in catalytic – domain structure and are specific to the brain, expressed in cortical neurons and hippocampal neurons respectively (Sato 1573). Together these kinases phosphorylate tau at 10 different phosphorylation sites, often catalytically relying on Mg^{2+} and Mn^{2+} cations to deposit the phosphate (Sato 1580). TTBK-1 and TTBK-2 are indeed identified as important targets for AD therapy, but no TTBK chemical inhibitors have been discovered nor synthesized to date.

Dual-Specificity Tyrosine-(Y)-Phosphorylation Regulated Kinase, or DYRK, is yet another non-proline directed protein kinase that has 6 different isoforms. The two isoforms actually involved in Alzheimer's disease are Dual-Specificity Tyrosine-(Y)-Phosphorylation Regulated Kinase-1A (DYRK1A) and Dual-Specificity Tyrosine-(Y)-Phosphorylation Regulated Kinase2 (DYRK2). Interestingly, chromosome 21 contains a gene on 21q22.2 which encodes DYRK1A; this is very important because chromosome 21 is involved in Down's syndrome and may be linked to the neurofibrillary tangles found within Down's syndrome patients (Martin 298). Both DYRK1A and DYRK2 phosphorylate tau protein but are relatively unique

regarding the other kinases mentioned in that they can prime other kinases to act with augmented efficiency. DYRKs are also able to undergo tyrosine auto-phosphorylation to achieve activation. One very potent chemical inhibitor is known, called Harmine.

Harmine, seen in Figure 15, is an alkaloid chemical that is also called Telepathine. It is a naturally occurring compound that is found in the Middle Eastern plant *Peganum harmala*. Its IUPAC name is 7-MeO-1-Me-9H-pyrido[3,4-b]-indole and has a molecular weight of 212.25 g/mol. It has a relatively small chemical structure composed mainly of three fused rings. Harmine is most commonly known for its ability to inhibit monoamine oxidase A (MAO-A), which is an enzyme that breaks down monoamine compounds. Some examples of monoamines are serotonin, norepinephrine, and psilocybin which are independently classified as a type of neurotransmitter, hormone, and recreational drug respectively. In addition to this effect, however, Harmine has been used as an anticancer as well as an inhibitor to DYRK1A. Harmine does in fact inhibit other DYRKs including DYRK2, but most effectively inhibits DYRK1A with an IC50 value of 80 nM (Martin 298).

Figure 15

Extracellular signal-regulated kinases (ERKs) are mitogen-activated protein kinases that are proline-directed. There are two isoforms, both of which are involved with AD: Extracellular signal-regulated kinase-1, or ERK1, and Extracellular signal-regulated kinase-2, or ERK2. They are also known as MAPK3 and MAPK1,

24

respectively. ERKs have one main activator and one main inhibitor, referred to as

Paclitaxel and FR180204 respectively.

Paclitaxel, seen in Figure 16, is a chemical activator of ERKs that is also

commonly referred to as Taxol or Onxal. Its IUPAC name is (2α,4α,5β,7β,10β,13α)-

4,10-Bis(acetyloxy)-13-{[(2R,3S)-3-

(benzoylamino)-2-hydroxy-3-

phen dihydroxy-9-oxo-5,20-epoxytax-11-

dihydroxy-9-oxo-5,20-epoxytax-11-

en-2-yl benzoate and is relatively
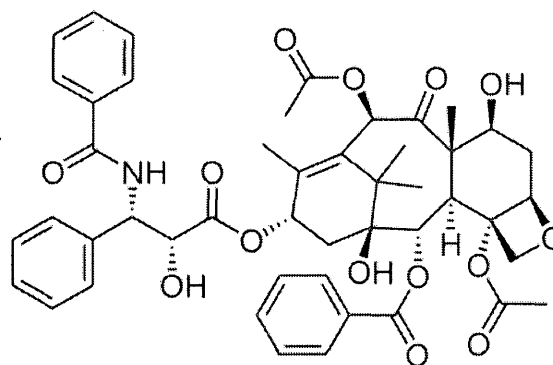
large in size compared with drugs

Figure 16

discussed so far. It is a naturally occurring compound, being isolated from tree bark of

the organism *Taxus brevifolia*, but is currently developed commercially after being

totally synthesized in 1994. Paclitaxel is most commonly known for its anticancer

properties, having been discovered officially in 1962 and thence utilized by the United

States National Cancer Institute and other Health Organizations. It is technically a

cytoskeleton toxin, as cells treated with the drug exhibit serious deficiencies in

chromosome segregation and mitotic cell division. This is because in addition to its

activation of ERK, which could lead to heightened phosphorylation and eventual

apoptosis, it over-stabilizes microtubule polymers by binding beta-tubulin microtubule

subunits (Lowe 1046). This microtubule stability seems like a positive attribute

regarding the reduction of cell death, but very stabilized microtubules have trouble

during disassembly, thus disrupting mitosis. Disrupted mitosis eventually leads to cell

death. Therefore, paclitaxel would definitely have the negative effects of cell death

that are situationally taken advantage of when fighting cancer, but if administered to a

person with AD, the microtubule stabilizing effects could be advantageous. Such

investigations into the efficacy of paclitaxel on neurodegenerative memory loss are

being conducted at institutions across the country, including The University of

Pennsylvania.

ERKs also have an inhibitor, named FR180204.

Its IPUAC name is 5-(2-Phenyl-pyrazolo[1,5-

a]pyridin-3-yl)-1H-pyrazolo[3,4-c]pyridazin-3-ylamine

and its molecular weight is 327.34 g/mol. FR180204 is

a potent inhibitor of ERK1 when compared to its

Figure 17

efficacy at inhibiting ERK2, with IC50 values of 0.310 micromolar and 0.806

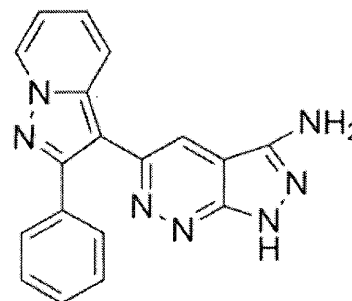micromolar respectively (Martin 298). FR180204 is portrayed by Figure 17.

P38s are mitogen-activated protein kinases that are involved in apoptosis and

differentiation of cells. There are four isoforms, p38- α, p38- β, p38- γ, p38- δ and are

referred to as MAPK14, MAPK11, MAPK12, and MAPK13 respectively. P38

phosphorylates tau at 21 different sites upon activation, which occurs via auto-

phosphorylation or in the presence of extracellular stress

(Martin 297). P38 has a potent inhibitor called SB-239063,

shown structurally in Figure 18.

Figure 18

SB-239063, or trans-4-[4-(4-Fluorophenyl)-5-(2-

methoxy-4-pyrimidinyl)-1H-imidazol-1-yl]cyclohexanol, is a

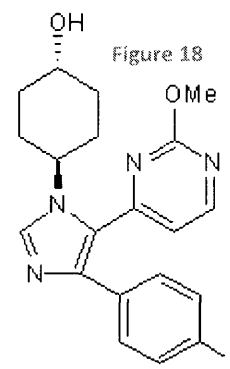selective inhibitor of p38 with an IC50 value of 0.044

micromolar and a molecular weight of 368.41 g/mol.

C-Jun N-terminal Protein Kinases (JNKs) are mitogen activated protein kinases (MAPK) with 10 different isoforms. The three main types which collectively house these ten isoforms are JNK1 (MAPK8), JNK 2 (MAPK9), and JNK 3(MAPK10). The first two are found in most tissues throughout the body including the brain, while JNK3 is almost exclusively found in brain tissue. JNKs range in size from 45 to 55 kDa and phosphorylate tau protein at 12 different sites, and is inhibited by protein phosphatases and especially by a chemical called SP600125 (Martin 297).

SP600125, shown in Figure 19, is a chemical inhibitor of the three aforementioned JNK types. Depicted to the right, its formal name is Anthra[1-9-cd]-pyrazol-6(2H)-one, but is more commonly referred to as 1,9-Pyrazoloanthrone or simply Anthrapyrazolone. This chemical has a molecular weight of 220.23 g/mol and has an IC50 value of 0.090 micromolar toward JNK3. It is very slightly more potent, however, at inhibiting JNK1 and JNK2 with respective IC50 values each at 0.04 micromolar (Martin 297).
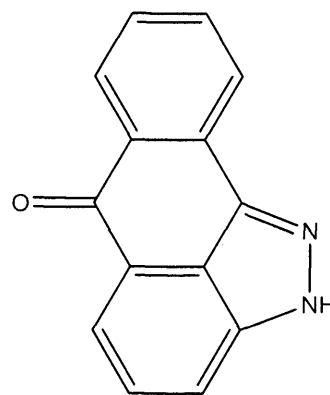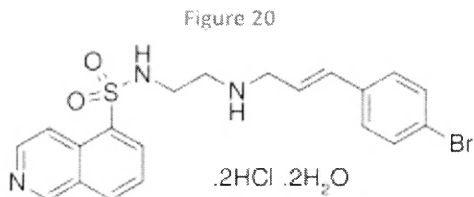
Figure 19

Protein Kinase A, or PKA, is an enzyme tetramer whose regulatory subunits require cyclic AMP, or cAMP, binding to induce enzymatic activation. It is for this reason that PKA is also commonly known as cAMP Dependent Protein Kinase. PKA phosphorylates 17 important sites along tau protein associated with AD brains, and

thusly can be considered an important target for AD therapy by inhibitors. The most important inhibitor of PKA activity is H-89 (Martin 299).

H-89, or N-[2-bromocinnamylamino)ethyl]-5-isoquinoline sulfonamide

Figure 20

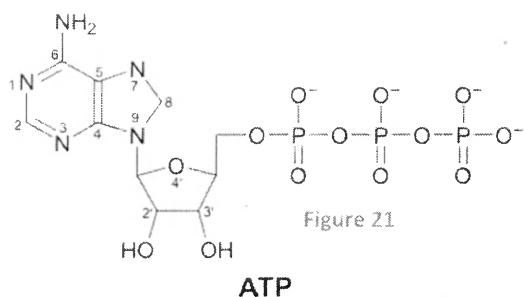dichloride hydrate, seen in Figure 20, is a potent PKA inhibitor with an interesting structure, roughly the size of an ATP molecule. Thusly, it inhibits PKA by acting in competition with ATP with isoquinoline mimicking adenosine, sulfonamide mimicking ribose, and bromobenzene mimicking the ATP

Figure 21

ATP

phosphates seen in Figure 21 (Lochner 265). The isoquinoline group of H-89 is certainly not the exact same size as the adenosine portion of ATP, but crystallography shows it is similar enough to bind PKA, in place of adenosine, around the amino acid Val 123 (Engh 876). After determining where the sulfonamide binds, Engh et al. attempted but were not able to
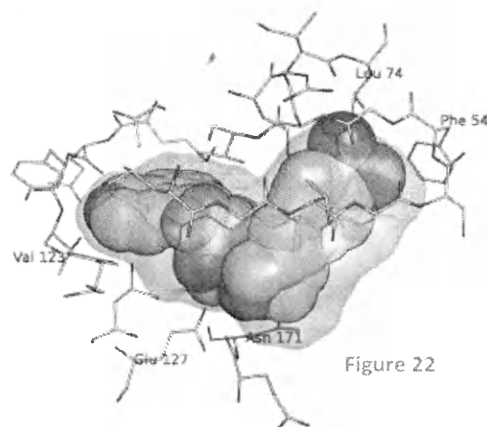

Figure 22

identify the exact crystallographic position of the bromobenzene electron density portion of H-89 binding, but they were in fact able to conclude that it was located roughly within the region where the ATP phosphates otherwise would bind. They depict the two best H-89 bindings to PKA in Figure 22.

Protein Kinase B, or PKB, is also known as Akt and has three main isoforms,

Protein Kinase B - α (PKB-α), Protein Kinase B - β (PKB-β), and Protein Kinase B - γ

(PKB-γ) or Akt-1, Akt-2, and Akt-3 respectively. PKB overexpression is known to

cause tau hyperphosphorylation at the main threonine and serine residues, threonine

212, serine 214, and 396 respectively (Martin 299). These three isoforms activate

GSK-3β and also have an inhibitor, Akt VIII trifluoroacetate hydrate salt.

Akt VIII, seen in Figure 23, inhibits all three isoforms but is more selective

toward Akt-1, with an IC50 value of 58 nM

compared to the larger 210nM IC50 value and

even larger 2100nM IC50 value for Akt-2 and

Akt-3. The salt is formally named 1,3-Dihydro-

1-(1-((4-(6-phenyl-1H-imidazo[4,5-

g]quinoxalin-7-yl)phenyl)methyl)-4-piperidinyl)-

2H-benzimidazol-2-one, corresponding to its

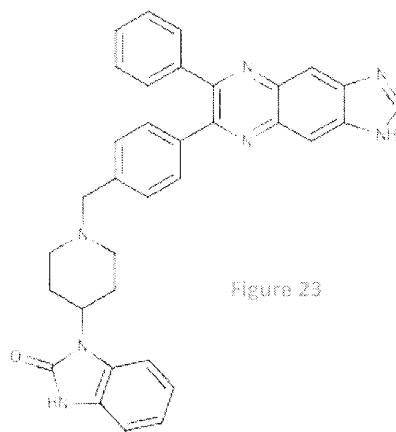large quinoxaline ringed chemical structure.

Figure 23

Interestingly, it is PKB specific in concentrations below 50 micromolar, but inhibits

PKA and PKC at concentrations above 50 micromolar (Martin 300).

Protein Kinase C, or PKC, is one of the most diverse protein kinases in that it

has over fifteen isoforms, but for simplicity, but can be classified into three broad

categories: conventional, novel, and atypical. Conventional PKCs include the four

isoforms PKC-α, PKC-β1, PKC-β2, and PKC-γ. These isoforms require DAG and

calcium ion to function. Novel PKCs include the seven isoforms PKC-δ, PKC-δ1,

PKC-δ2, PKC-δ3, PKC-ε, PKC-η, and PKC-θ. These novel isoforms require DAG but

do not require calcium ion to function. The remaining five isoforms that are referred to

as atypical include the following: PKC-ι, PKC-ζ, PK-N1, PK-N2, and finally, PK-N3.

These five are referred to as such because they are not like the rest, for they require

neither calcium ion nor DAG to function. In my model, DAG is incorporated

mathematically as an activator as it is required by the majority of PKC isoforms to

function. Bisindolylmaleimide I is also incorporated, as it is a potent chemical

inhibitor of PKC (Martin 300).

Diacylglycerol, or DAG, seen in Figure 24, is from a fundamental biological

perspective is a type of molecule also called diglyceride that is involved in

Figure 24
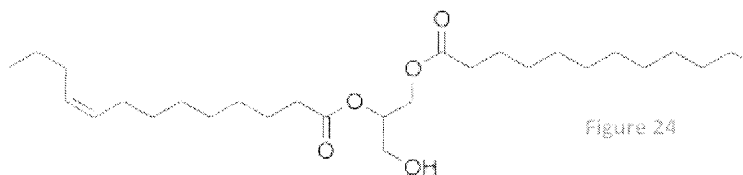
biochemical signaling of secondary messages. One particular DAG involved in PKC

signaling is a long lipid that is formally called 1-palmitoyl-2-oleoyl-glycerol. The

DAG is found in the cell membrane, and the conventional and novel PKCs bind DAG

to achieve activation and thence ability to phosphorylate substrate, such as Tau

protein. If the PKC is indeed conventional, calcium ions from the inositol

triphosphate, or IP_3, intermembrane channel belonging to the endoplasmic reticulum

will need to be provided via release into the cytosol. IP_3 is a chemical that will always

be present as long as DAG is present in the cell membrane, because it is a byproduct

of Phospholipase C, which is an enzyme that cleaves IP_3 from phosphatidylinositol

4,5-bisphosphate, or PIP_2, to form DAG fundamentally. Ligands need to bind a

surface receptor to stimulate this entire pathway secondary messenger signaling

pathway.

Bisindolylmaleimide I, or

GF-1, seen in Figure 25 is a

chemical inhibitor of PKC. Its

formal name is 3-[1-[3-

(dimethylamino)propyl]-1H-indol-

3-yl]-4-(1H-indol-3-yl)-1H-

pyrrole-2,5-dione and the chemical

has a truly fascinating structure
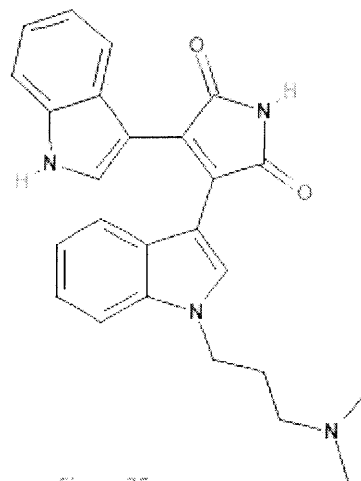
with near symmetrical dual indole

Figure 25

substituents coming off of a main unsaturated double γ-lactam. GF-1 is a potent

inhibitor of the conventional PKCs with IC50 values less than 21 nM. It can also

inhibit the novel PKCs, exhibiting IC50 values below 200 nM. It does not do well

with the atypical PKCs, whereas GF-1 is only able to inhibit 50% of PKC-ζ with a

concentration of 5800 nM (Martin

300). Another important modulator

of PKC activity is Bryostatin 1,

seen in Figure 26.

Figure 26

Bryostatins are very large

lactones that inhibit PKC.

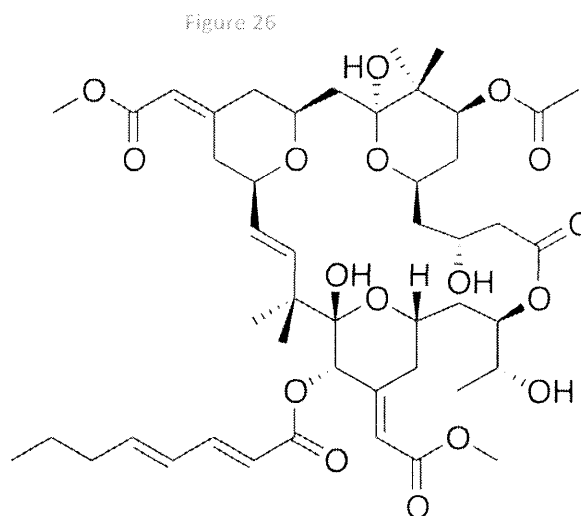Originally, Bryostatins were

naturally isolated from the *Bugula*

31

neritina, which are a species of aquatic invertebrates called bryozoan. There are currently over 19 Bryostatins that have been isolated or synthesized. They were first employed as anti-cancer agents, but are to date being investigated in neurodegenerative diseases such as Alzheimer's disease. Bryostatin 1, involved in AD, has the formal name (1S,3S,5Z,7R,8E,11S,12S,13E,15S,17R,20R,23R,25S) -25-Acetoxy-1,11,20-trihydroxy-17-[(1R)-1-hydroxyethyl]-5,13-bis(2-methoxy-2-oxoethylidene)-10,10,26,26-tetramethyl-19-oxo-18,27,28,29-tetraoxatetracyclo-[21.3.1.13,7.111,15] nonacos-8-en-12-yl (2E,4E)-2,4-octadienoate.

There are other kinases of course, but these are the ones that I have targeted as having the highest potential for proving therapeutic regarding the treatment of Alzheimer's disease.

Molecules involved in the phosphatase pathway:

Protein Phosphatase 2 (PP2A) was mentioned with regards to zinc and the casein kinases above, but not fully explored. This protein is directly involved in removing phosphate groups from proteins like Tau at the serine and threonine residue regions; therefore, it is a catalyst of tau dephosphorylation. It has been shown to be upregulated by lithium in the rat frontal cortex and hippocampus (Tsuji 413). It is heterotrimeric in structure, comprised of a heterodimeric core enzyme and a subunit that provides regulation. The heterodimeric portion is comprised of a catalytic subunit and a scaffolding subunit, respectively, in addition to being supported by Mg^{2+} coenzyme (Xu 1239).

PP2A is the major tau phosphatase in the

brain but should be used with caution as it is

more broad in its substrate specificities than

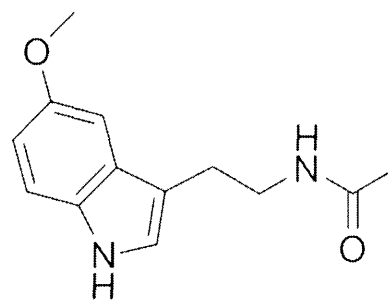protein kinase inhibitors, which could lead to

Figure 27

negative, unforeseen side effects (Gong 2326). Two inhibitors regulate PP2A activity,

known as I_1^{PP2A} and I_2^{PP2A} respectively. Melatonin, seen in Figure 27, is otherwise

known as N-acetyl-5-methoxytryptamine or N-[2-(5-methoxy-1H-indol-3-yl)ethyl],

and acts in a reverse manner and thus restoring PP2A activity (Gong 2327). However,

melatonin could have other side effects upon tau hyperphosphorylation reversal due to

its widespread hormonal abilities that have been prescribed to treat or subdue

circadian rhythm sleep disorders, immune disorders, and cardiovascular disorders, as

well as sexual dysfunction.

Okadaic acid seen in Figure 28, is a well-known marine-derived toxin named

after the species *Halichondria okadai*, a type of sea sponge. It is a relatively large

molecule that is in fact produced by algae and plankton. It is formally a toxin with
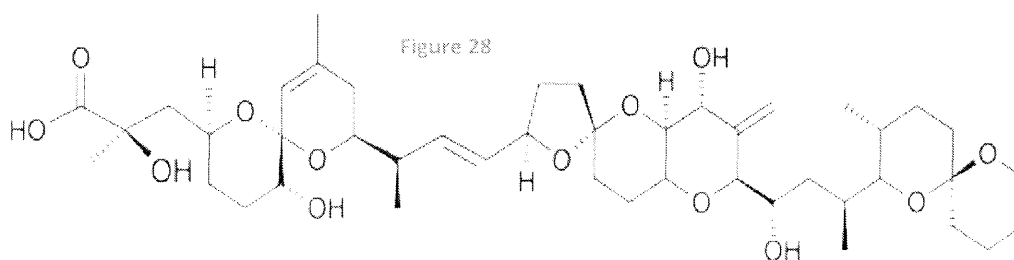

Figure 28

chemical name (2R)-3-[(2S,6R,8S,11R)-2-[(E,1R)-3-[(2S,2&primeR,4R,4aS,6R,8aR)-

4-hydroxy-2-[(1S,3S)-1-hydroxy-3-[(2S,3R,6S)-3-methyl-1,7-dioxaspiro[5.5]undecan-

2-yl]butyl]-3-methylene-spiro[4a,7,8,8a-tetrahydro-4H-pyrano[2,3-e]pyran-6,5'-

tetrahydrofuran]-2'-yl]-1-methyl-prop-2-enyl]-11-hydroxy-4-methy-l-1,7-

dioxaspiro[5.5]undec-4-en-8-yl]-2-hydroxy-2-methyl-propanoic acid. Okadaic acid

33

does not act directly on tau protein, but mathematically has the same effect as tau

phosphorylation by instead acting to non-competitively inhibit PPA2. Upon ingestion

of the toxin, in addition to the inhibition of Ser/Thr phosphatases such as PP2A in

places like brain hippocampal neurons, Okadaic acid causes diarrheal shellfish

poisoning, or DSP (Kamat 164). This occurs in the intestinal tract, in which Okadaic

acid inhibits the removal of phosphate to induce more permeability along

gastrointestinal cell membranes, hence diarrhea as a symptom. One chemical which

seems able to reverse the negative effects of Okadaic acid is memantine.

Memantine is an N-methyl-D-aspartate , or

NMDA, receptor agonist that modulates PP2A

signaling. Its IUPAC name is 3,5-

dimethyltricyclo[3.3.1.13,7]decan-1amine and is

named such because of the triple fused saturated ring

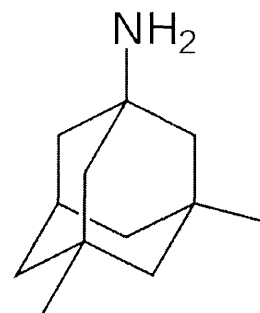system seen to the right in Figure 29.

Figure 29

It blocks over-activated NMDA receptors and thus prevents excite-toxicity (Li

268). In moderate to severe AD, memantine prevents tau hyperphosphorylation in

hippocampal neurons (Gong 2324).

METHODS

A simplified model of Alzheimer's disease was made via the program Cell

Designer4.2 using tau protein literature regarding molecular links to

hyperphosphorylation. Below, in Figures 31 and 32, are snapshots of two of the most

important processes in the graduate student version of the model. They are not true

Figure 30
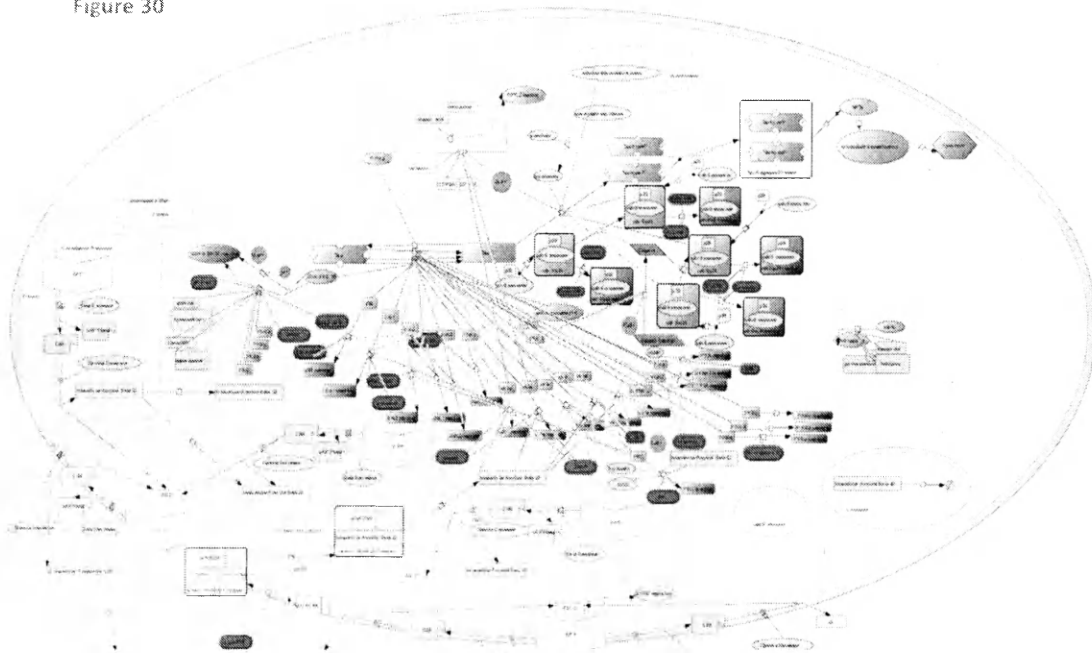
snapshots, but rather cleaned up versions because the real model has become so

complex that it is difficult to visually interpret, as evident in Figure 30 above.
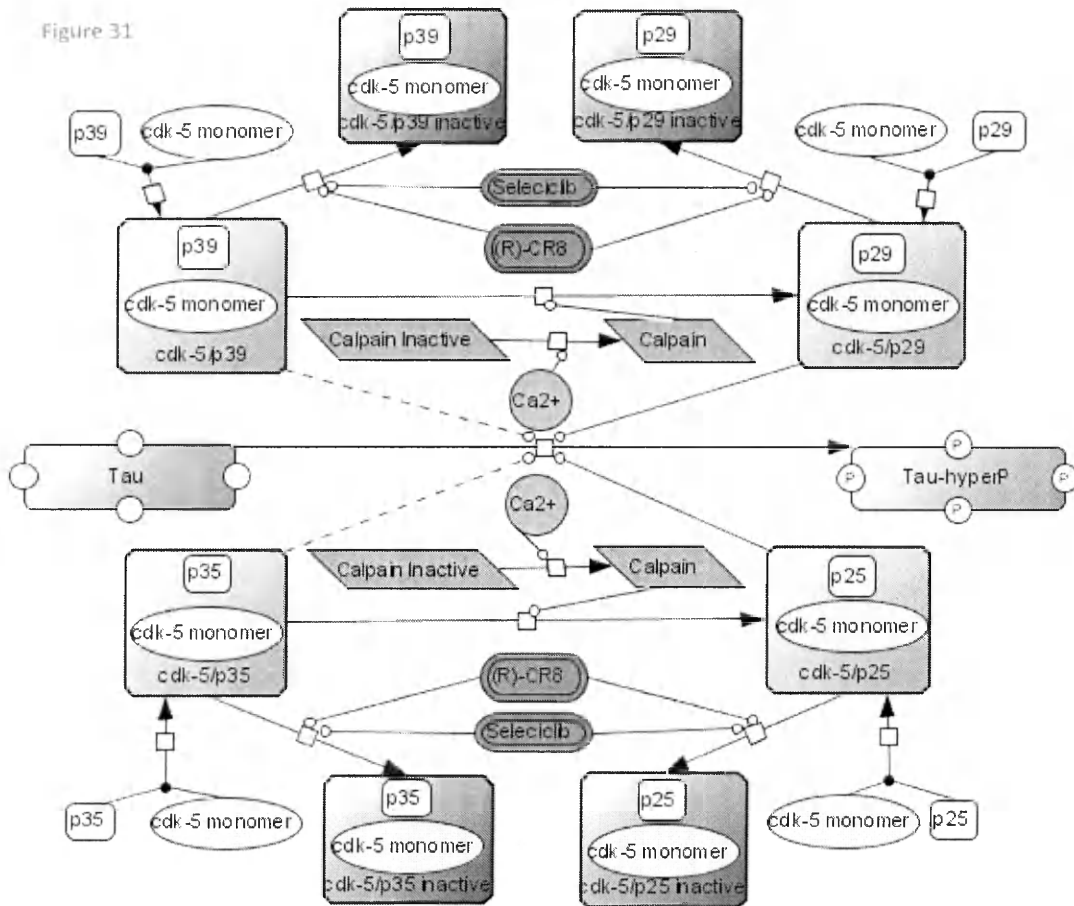
Figure 31

As seen here in Figure 31, CDK-5 complexes of four varieties

hyperphosphorylate Tau protein. Generally throughout the whole model, the dark

green as seen here is consistent with the color for all of the tau protein kinases, and the

dark blue also as seen here is consistent with the inactive forms of said kinases. The

shiny red color of the tau proteins here is consistent with the entire pathway from tau

to NFT formation, microtubule destabilization, and ultimately apoptosis. Lines that

join to form a single filled arrow were chosen to be indicative of heterodimer

association or complex formation. Other regular filled arrows were chosen to be

indicative of transition states from molecule to molecule, whereas lines with unfilled

circular ends were chosen to be indicative of activation. The caveat here is that the

molecules exhibiting lines with unfilled circular ends activating the process of

36

inactivation were later integrated as inhibitors of the species undergoing said inactivation. This is seen, as one might expect, with R-CR8 and Seleciclib. They are both chemical inhibitors of the four CDK-5 complexes, but it was more convenient in CellDesigner to portray them as activating the process of kinase inactivation.
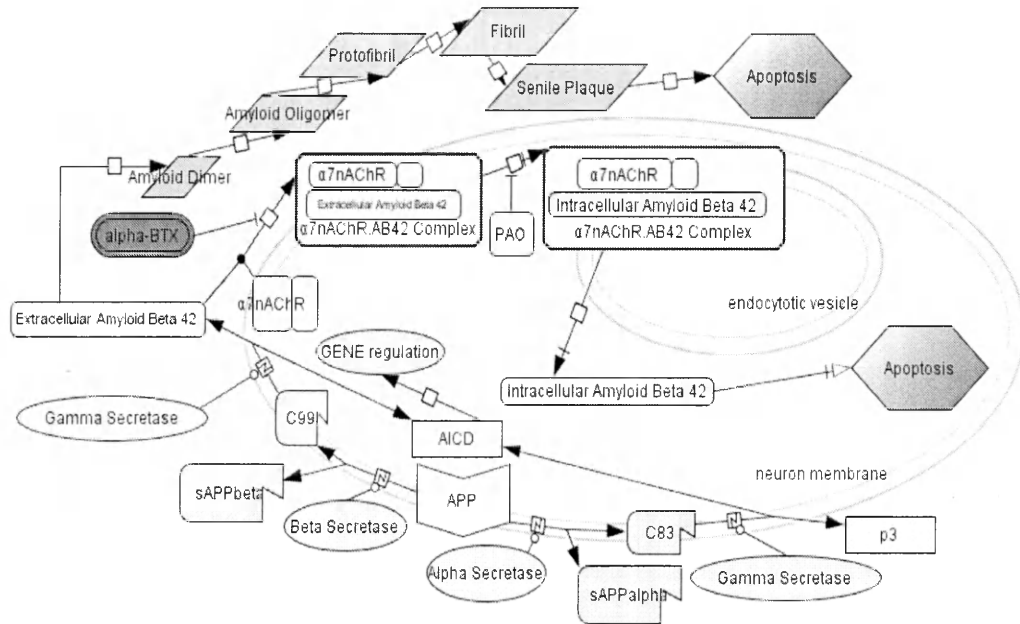

Figure 32

As seen here in Figure 32, the non-amyloidogenic pathway to the right of APP and the amyloidogenic pathway to the left of APP, resulting in aforementioned Extracellular Amyloid Beta 42 and eventual apoptosis via the senile plaque formation cascade. The senile plaque cascade is portrayed in lime green while the extracellular secretases are in a softer green. The amyloid is internalized via complex formation and endocytotic vesicle transport throughout the cell. The resultant intracellular amyloid then leads to the tau hyperphosphorylation pathway, thus triggering apoptosis. The trigger arrow is the type with an unfilled arrowhead and perpendicular line just beneath the arrowhead, signifying that there are aforementioned molecular pathways

taken in between to reach the molecule or process being triggered. The transport arrow looks the exact same as the trigger arrow, but it has a filled arrowhead. The inhibitor 'arrow' is not quite an arrow as much as a line with a small perpendicular end. It is seen regarding bungarotoxin and PAO above.

After the molecular modeling, Biological Systems Theory (BST) was used to make sense of the above complexity exhibited by the model as a whole. Originally developed by Eberhard Voit, BST allows theoretical biochemists to use ordinary differential equations to model cell activity mathematically. Our group employed many of the same BST methods described in a previous Coleman group, Sass et al. (2009), but the main difference is that ours used Michaelis equations, Hill equations, and real numerical values as inputs instead of theorized estimated values for the first time ever. We also used the more current and updated program MATLAB version R2014a instead of PLAS.

To acquire these values and thereby mathematically model the neuron with true, real-life accuracy, large databases of proteins and drugs alike such as BRENDA and MOPED were scoured that ultimately resulted in a whole spreadsheet full of formal name listings, LC50 values, IC50 values, initial concentrations, and rate constant values. Most of the time, these values were found cited as being from frontal lobe brain tissue, which was especially helpful.

With a full set of values and coded system of equations, our group set out to find the specific set of drug concentrations which would be therapeutic in reducing the amount of tau protein hyperphosphorylation and thereby a theoretical treatment for

Alzheimer's disease. Computational healthy cell and diseased cell states were

constructed, then drugs were selected.

Figure 34 below is a snapshot of the Hill equations implemented. Each line of

code after the 'death=' portion is for a specific drug, utilizing a specific LD50 value.

These Hill equation variants are of the form

$1/(1+e^\wedge(Tox-[Drug]))$, where tox=LD50 and

Drug is the drug concentration from the list in

Figure 33 that uses dynamic_concentration as a

tool for calling from said list. Drugs taken into

account here were SP-600125, R-CR8, 6-BIO,

AR-A014418, SB-239063, paclitaxel, heparin,

bryostatin, harmine, seleciclib, and alpha BTX.

Other drugs were not included for various

reasons, ranging from our group deeming them

as drugs that are unfit for this study or simply

ones where LD50 values do not currently exist in

Figure 33

```
X(134)  = 90;  %SP 600125
X(135)  = 130;  %(R)-CR8
X(136)  = 5;  %6-BIO
X(137)  = 104;  %AR-014418
X(138)  = 44;  %SB-239063
X(139)  = 310;  %FR-180204
X(140)  = 1000;  %paclitaxel
X(141)  = 110;  %TBCA
X(142)  = 660;  %Heparin
X(143)  = 160;  %IC261
%X(144)  = 5300;  %GF1
X(145)  = 80;  %harmine
%X(146)  = 2100;  %AKT inhibi
X(147)  = 50;  %H-89
X(148)  = 280;  %seleciclib
    Xind(51)  = 1500;  %-Xind
X(149)  = 10;  %-X(149) = nym
X(150)  = 40;  %-X(150) = fla
X(151)  = 1.9;  %-X(151) = st
X(152)  = 281;  %X(152) = Bry
X(153)  = 0.54;  %X(153) = al
X(154)  = 0.858;  %alcisine
```

the literature due to lack of clinical trial testing. The beauty here is that different drugs

can easily be added or subtracted from the equation when the need presents itself or

when one wants to change the parameters of the study. Ultimately this set of equations

uses lethality data to produce a semi-sigmoidal dose-response curve for every single

drug incorporated into the equation set.

Figure 34

```
drug_params;
    init_opt=X;
    topt=[0,300];
    [times,dynamic_concentrations]=ode45(@model,topt,init_opt);
    %plot(times,dynamic_concentrations)
    [len,width]=size(dynamic_concentrations);
    death= 1/(1+2.71828^(((18.18181818*10^3)-dynamic_concentrations(len,99))*1/((18.181
    1/(1+2.71828^((2500-dynamic_concentrations(len,134))*1/(2500/4)))+ ...% SP-600...
    1/(1+2.71828^(((6.96*10^6)-dynamic_concentrations(len,135))*1/(6.96*10^6/4)))+ ...%
    1/(1+2.71828^((9000-dynamic_concentrations(len,136))*1/(9000/4)))+ ...%Kee 6510*dyr
    1/(1+2.71828^(((320910)-dynamic_concentrations(len,137))*1/(320910/4)))+ ...%Kee_SP
    1/(1+2.71828^(((6921.82)-dynamic_concentrations(len,138))*1/(6921.82/4)))+ ...%Kee_
    1/(1+2.71828^(((38857.71)-dynamic_concentrations(len,140))*1/(38857.71/4)))+ ...%Ke
    1/(1+2.71828^(((211555)-dynamic_concentrations(len,142))*1/(211555/4)))- ...%Kee_be
    1/(1+2.71828^(((1.17*10^6)-dynamic_concentrations(len,145))*1/(1.17*10^6/4)))+ ...%
    1/(1+2.71828^(((1.01*10^6)-dynamic_concentrations(len,148))*1/(1.01*10^6/4)))+ ...%
    1/(1+2.71828^(((2.62*10^9)-dynamic_concentrations(len,149))*1/(2.62*10^9/4)))+ ...%
    1/(1+2.71828^(((2.81*10^9)-dynamic_concentrations(len,150))*1/(2.81*10^9/4)))+ ...%
    1/(1+2.71828^(((1.23*10^7)-dynamic_concentrations(len,151))*1/(1.23*10^7/4)))+ ...%
    1/(1+2.71828^(((76.64)-dynamic_concentrations(len,152))*1/(76.24/4)))+ ...%Kee_bryc
    1/(1+2.71828^(((10.22)-dynamic_concentrations(len,153))*1/(10.22/4)))+...%- ...%Kee
    1/(1+2.71828^(((5.723*10^6)-dynamic_concentrations(len,154))*1/(5.723*10^6/4)))...%
```

Figure 35 below is a sample snapshot of how michaelis menten kinetics

variants were used to mathematically model the enzyme catalyzed tau

phosphorylation. Km ATPs were used instead of Km tau for simplicity purposes.

Almost every line in the code here represents a kinase that is acting on tau protein.

Equation portions with irrational e's in them represent the drugs acting on the kinases,

which can be easily turned on and off via commenting and uncommenting in

MATLAB syntax '%' to produce a variety of different data regarding the changing

variable of interest, which in this figure is hyperphosphorylated tau arbitrarily valled

variable X(99).

Figure 35

```
dX(99) = 0.0180915079*X(100)*(((0.00017035*X(101))/(1.4*10^3+X(100))*(
+(0.0979767795*Xind(1)/(1.0*10^3+X(100)))... %ITBK1
+(0.00000189212*Xind(2)/(14*10^3+X(100)))... % ITBK2          KK: 137,4.
+ ((0.021455*X(135)/(2.7*10^3+X(100)))*(1/(1+e^((X(139)-44)*(1/(44/4)))
+ ((0.0014*X(103)/(3.4*10^3+X(100)))*(1/(1+e^((X(134)-90)*(1/(90/4))))
+ (((0.0092*X(104))/(1.7*10^3+X(100)))*(1/(1+e^((X(140)-1000)*(1/(1000,
+ ((0.0568*(X(105))/(1*10^3+X(100)))*(1/(1+e^((X(134)-90)*(1/(90/4))))
+ (((0.0193*X(106))/(1.4*10^3+X(100)))*(1/(1+e^((X(134)-90)*(1/(90/4))
+ (((0.00246*X(107))/(390+X(100)))*(1/(1+e^((X(134)-90)*(1/(90/4)))))
+ (((0.0000261256*X(108))/(200+X(100)))*(1/(1+e^((X(142)-660)*(1/(660/·
+ (((0.0052192067*X(109))/(3900+X(100)))*(1/(1+e^((X(142)-660)*(1/(660,
+ ((0.0006388899*X(110))/(1600+X(100))) ...      %Klepsilon
+ ((0.003795424*X(111))/(7700+X(100))) ...       %Kldelta
+ ((0.0004518072*X(112))/(4100+X(100))) ...      %Klalpha
+ (((0.0342093023*X(113))/(16000+X(100)))*(1/(1+e^((X(145)-80)*(1/(80/·
+ (((0.0187541259*X(114))/(7700+X(100)))*(1/(1+e^((X(145)-80)*(1/(80/4)
+ ((0.0050574713*X(115))/(4220+X(100)))...
+ ((0.0035858359*X(116))/(87900+X(100)))...
+ ((0.0023310441*X(117))/(358400+X(100)))...
+ ((0.00555*X(118))/(41000+X(100)))...
+ (((0.00686*X(119))/(2400+X(100)))*(1/(1+e^((X(152)-281)*(1/(281/4))),
+ (((0.00008675284*X(120))/(0.2*10^3+X(100)))*(1/(1+e^((X(135)-130)*(1,
+ (((0.00017587249*X(121))/(1.8*10^3+X(100)))*(1/(1+e^((X(135)-130)*(1,
- ((0.00260234486*Kind(106))/(11.6*10^3+X(99)))*X(99);
```

To control the parameters of the plots generated from the combined death

function equations and michaelis kinetics equations incorporated into the code, an

advanced plotting tool seen in Figure 35 was utilized, as seen partially in the snapshot

Figure 36 below. The "+, o, *, etc" are all strings used to denote different drugs,

assigned arbitrarily as the plotter receives them, allowing us to distinguish one drug

from another drug. The most important portions of this code are the resolution and the

range.

The resolution is essentially the number of points that are plotted,

appropriately giving enhanced resolution when this number is increased. This is

especially important for plots which do not appear contiguous upon initial inspection;

the resolution can be increased to reveal the activity of the drug in areas unclear on the

graph. The catch here is that for every order of magnitude one increases resolution, the

computational time for generating the plot of interest increases proportionally. This

leads to some intensely long sessions of plotting just to make sure some drugs do not

have extraneous local minimum cell death Y-axis values that do not initially appear.

Figure 36

```
style=['-','o','*','.','x','s','d','^','v','>','<','p','h',...
    '-','o','*','.','x','s','d','^','v','>','<','p','h',...
    '-','o','*','.','x','s','d','^','v','>','<','p','h',...
    '-','o','*','.','x','s','d','^','v','>','<','p','h'];
resolution=1000;
val_multiplier=linspace(0,7,resolution); %does range 0 to multiplier
X_g=zeros(resolution,15);
Y_g=zeros(resolution,15);
xvalues=linspace(0,50000,resolution); %con
for i=[14]
    for j=1:resolution
        xval=val_multiplier(j)*drug_initials(i); %picks xvalues based on
        %xval=xvalues(j);
        drug_used=drug_params;
        drug_used(i)=xval;
        yval=death_output(drug_used);
        X_g(j,i)=xval;
        Y_g(j,i)=yval;
        %X_g(j)=xval;
        %Y_g(j)=yval;

        legend_entry(i)=plot(X_g(j,i),Y_g(j,i),style(i),'color',colors(i,:));
        %use otherwise

        %plot(X_g(j,i),specs(1),style(i),'color',colors(i
        % plot(X_g(j,i),specs(2),'k-');
        %justassigned;
    end
end
```

The range is simply computed using "xvalues=linspace(0,15000,resolution)"

but can also be computed using "val_multiplier=linspace(0,7,resolution);", which

essentially automatically chooses a range from 0 to a multiplier of the drug's IC50

value, in this case being 7 times. Changing the 0 and 15000 values in the first case

simply determines the concentration of the drug on the X-axis. This allows one to

instantly locate the region of the graph where the supposed LD50 value is and make

sure it is behaving properly. The range also works in tandem with the resolution, for

42

when the range is shortened more data can be plotted without changing the resolution

to a higher, computationally expensive value. The key here is to use both the

resolution and the range as efficiently as possible to find apoptosis minima.

RESULTS

The following Figures 37 – 58 are the results gathered from MATLAB plotting

functions. Figures 37 and 38 show constructed healthy and diseased states, while

Figures 39 – 57 show graphs of the selected drugs with concentration versus apoptosis

relative value. Figure 58 is essentially a table with all of the important data tabulated

and further discussed in the discussion section.

Figure 37: Healthy State
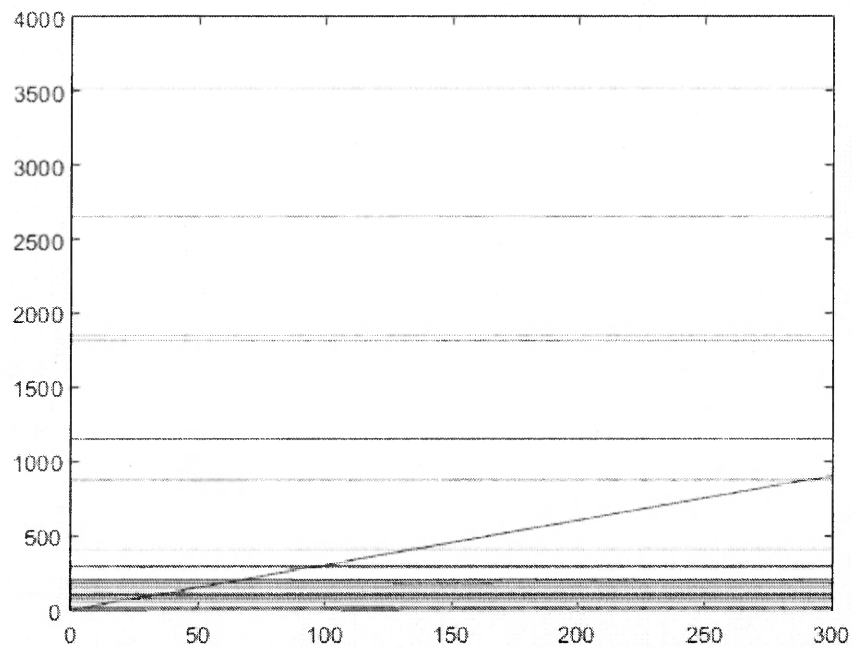
Figure 38: Diseased State
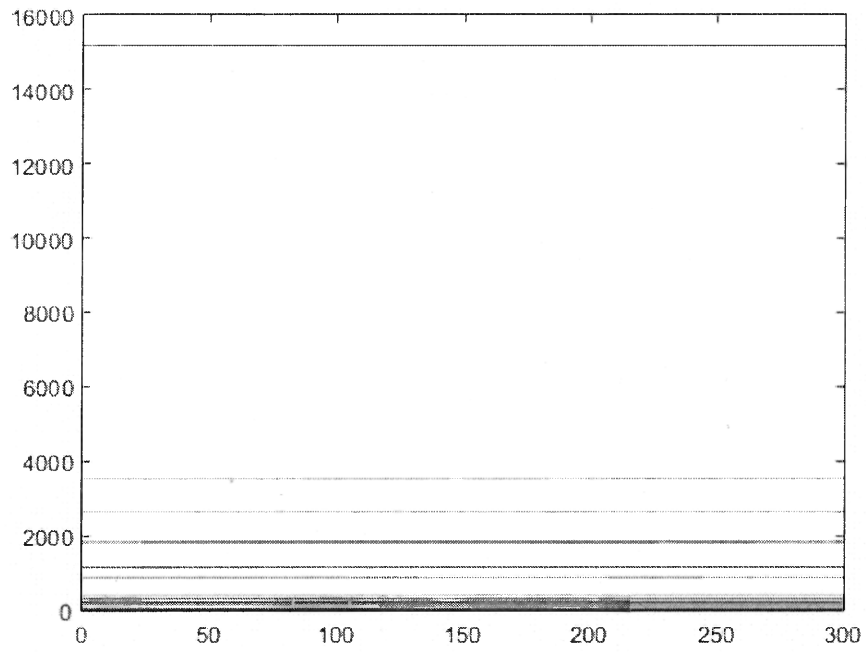
Drugs Plotted with Concentration(nM) versus Apoptosis

SP-600125 Plots

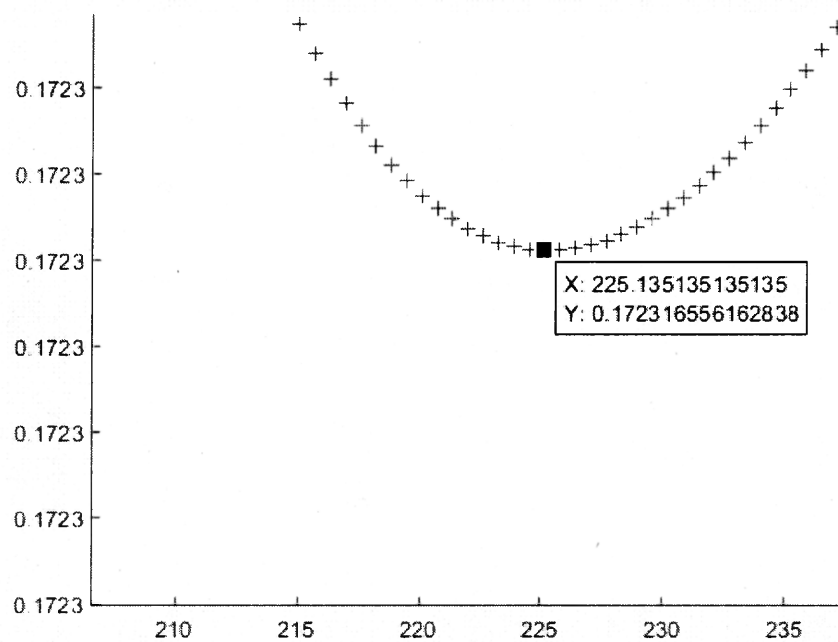## Figure 39: SP-600125 Concentration Range 0:700 nM (~7x IC50)
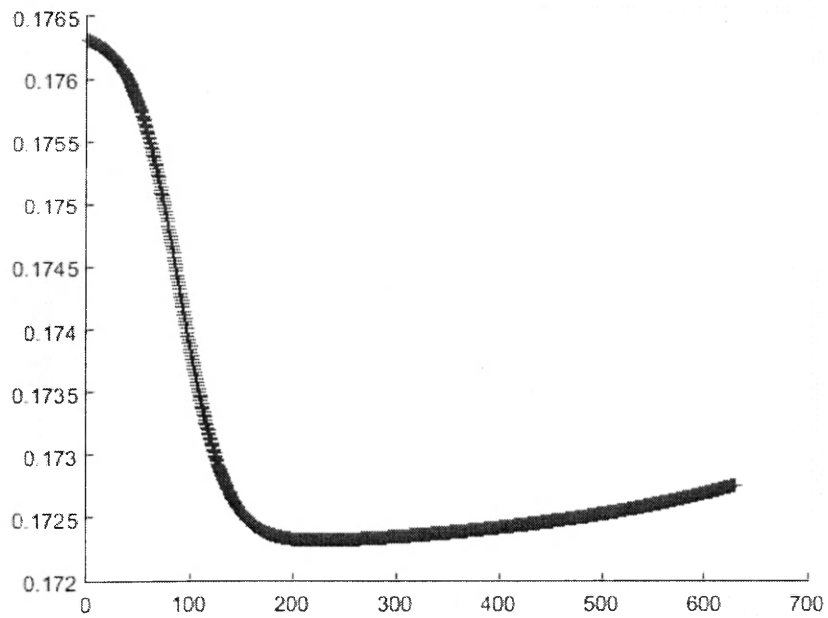
Figure 40: SP-600125 Concentration Range 210:235 nM with minimum

X: 225.135135135135
Y: 0.172316556162838

(R)-CR8 Plots

Figure 41: (R)-CR8 Concentration Range 0:900 nM (~7x IC50)
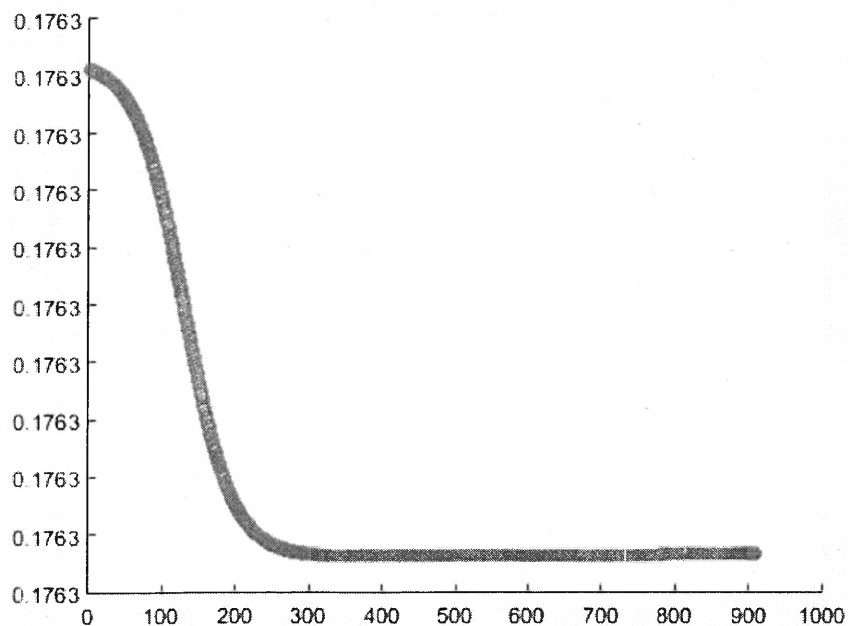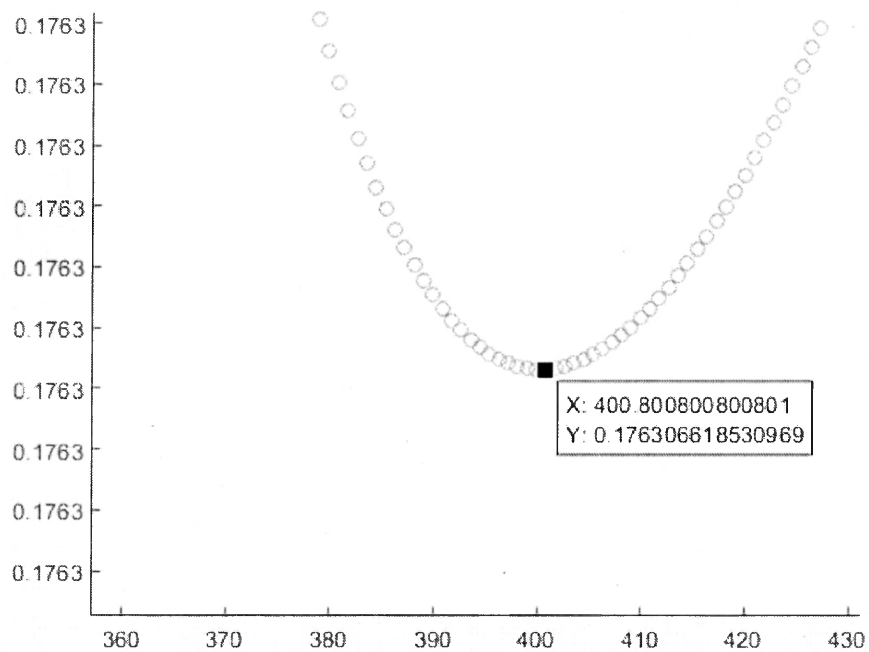
Figure 42: (R)-CR8 Concentration Range 360:430 nM with minimum

6-BIO Plots
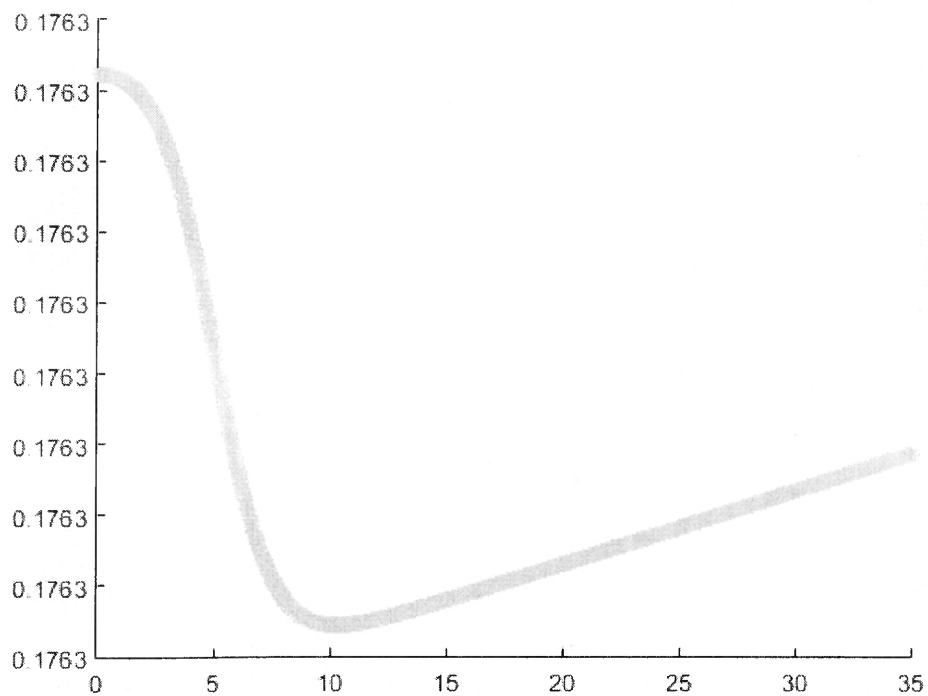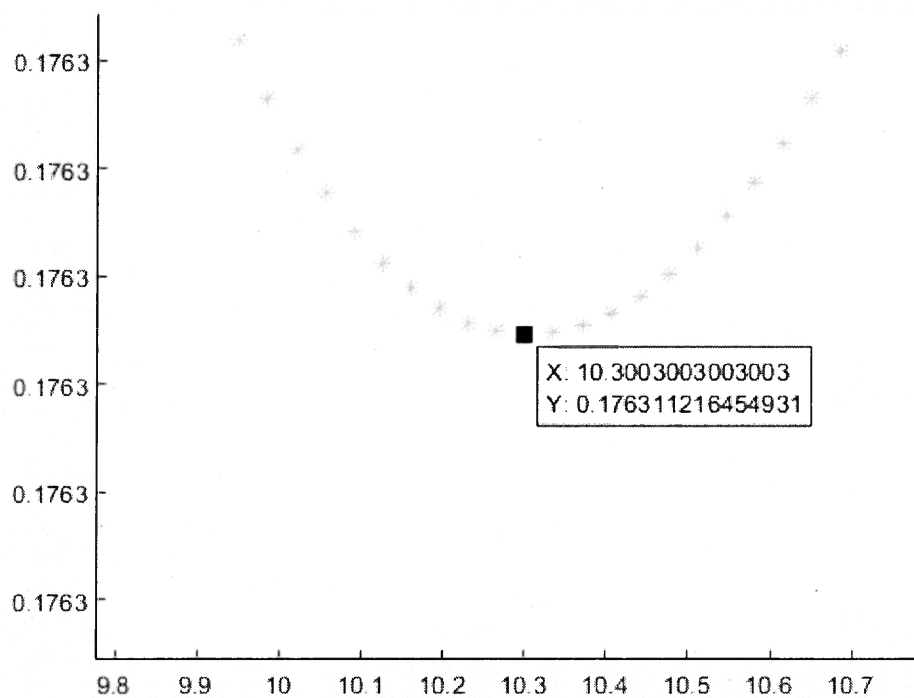
Figure 43: 6-BIO Concentration Range 0:35 nM (~7x IC50)

Figure 44: 6-BIO Concentration Range 9.8:10.7 nM with minimum

X: 10.3003003003003
Y: 0.176311216454931

AR014418 Plots

Figure 45: AR014418 Concentration Range 0:800 (~7x IC50)
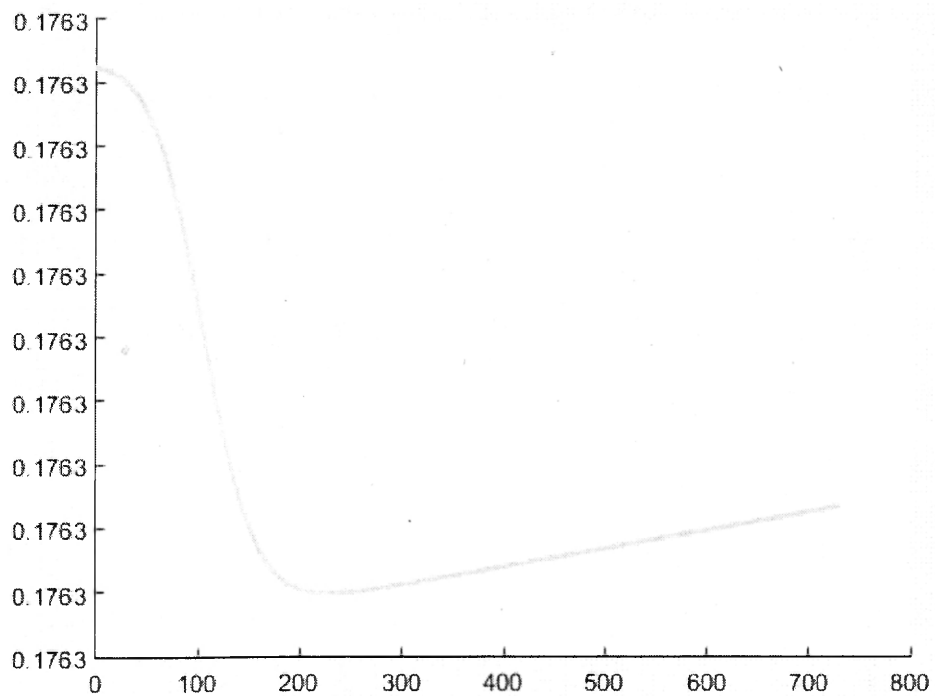
Figure 46: AR014418 Concentration Range 220:245 nM with minimum

X: 228.820820820821
Y: 0.176310991149103
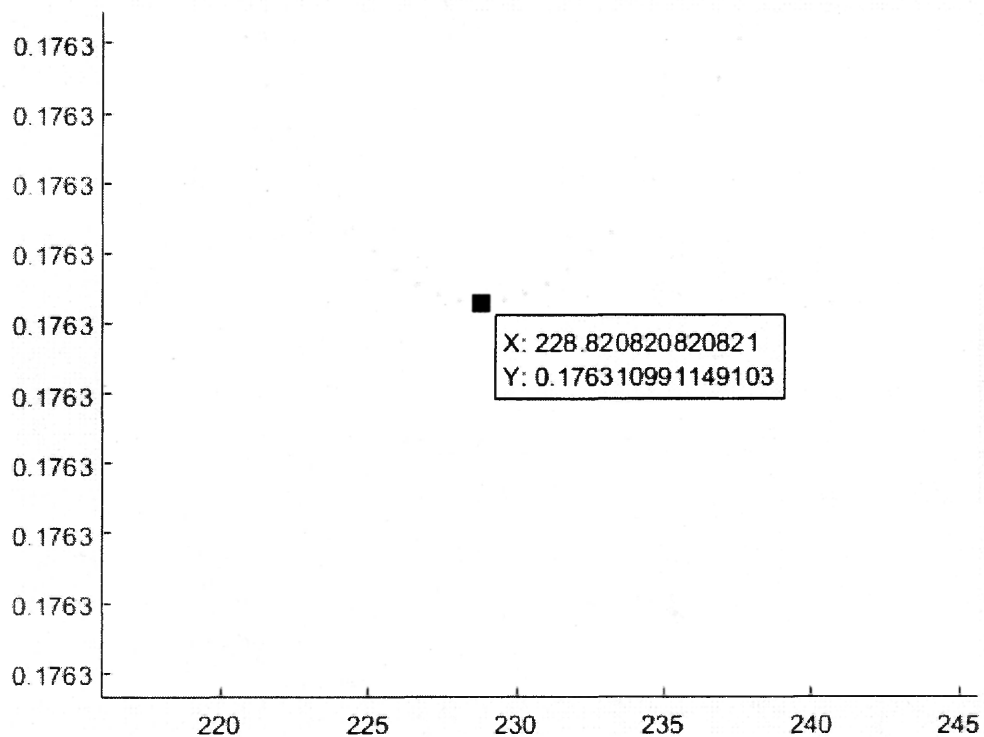
SB-239063 Plots

Figure 47: SB-239063 Concentration Range 0:4500 (not effective)
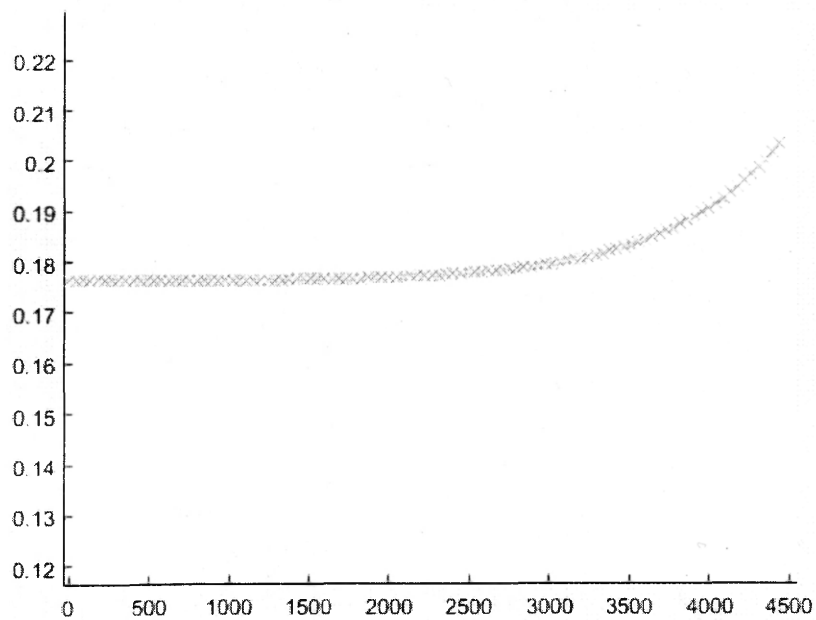
Paclitaxel Derivative (Hypothetical) Plots

Figure 48: Paclitaxel Derivative Concentration Range 0:8000 (~x25 IC50)
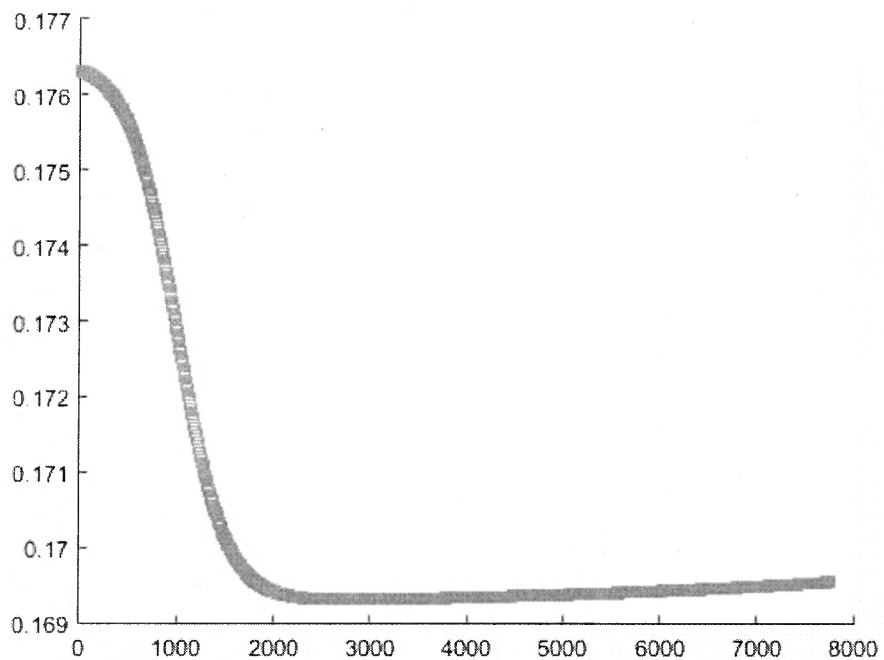
Figure 49: Paclitaxel Derivative Concentration Range 2650:2900 with minimum

X: 2769.51951951952
Y: 0.169304606955883
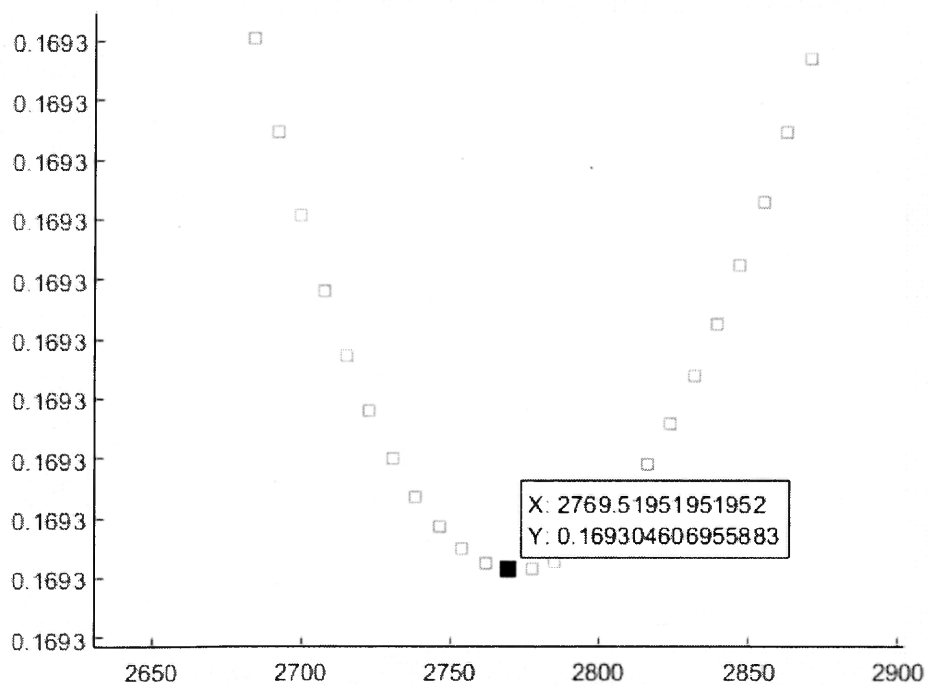
Heparin Plots

Figure 50: Heparin Concentration Range 0:7000
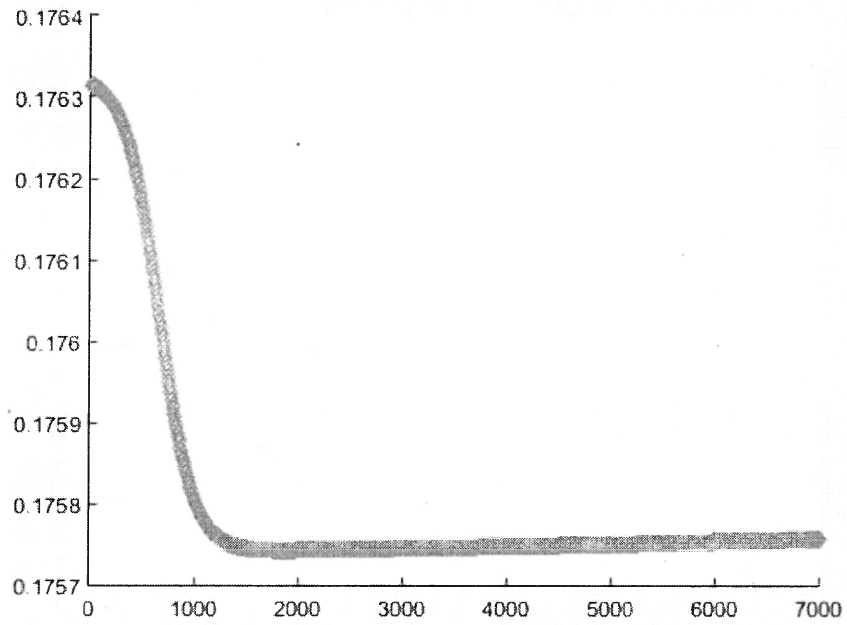
Figure 51: Heparin Concentration Range 1650:2150 with minimum

X: 1870.87087087087
Y: 0.175742774884029
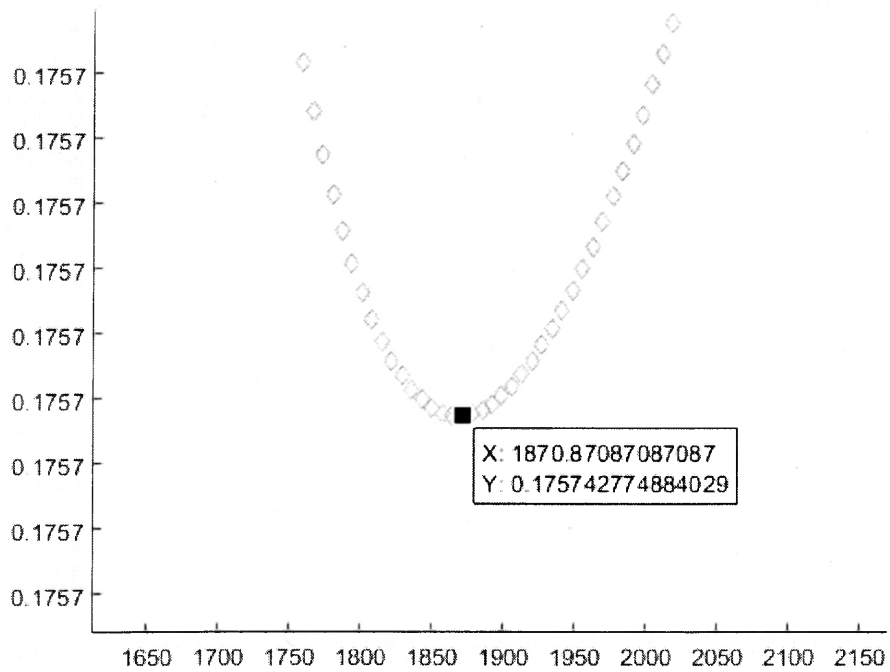
Harmine Plots

Figure 52: Harmine Concentration Range 0:5000
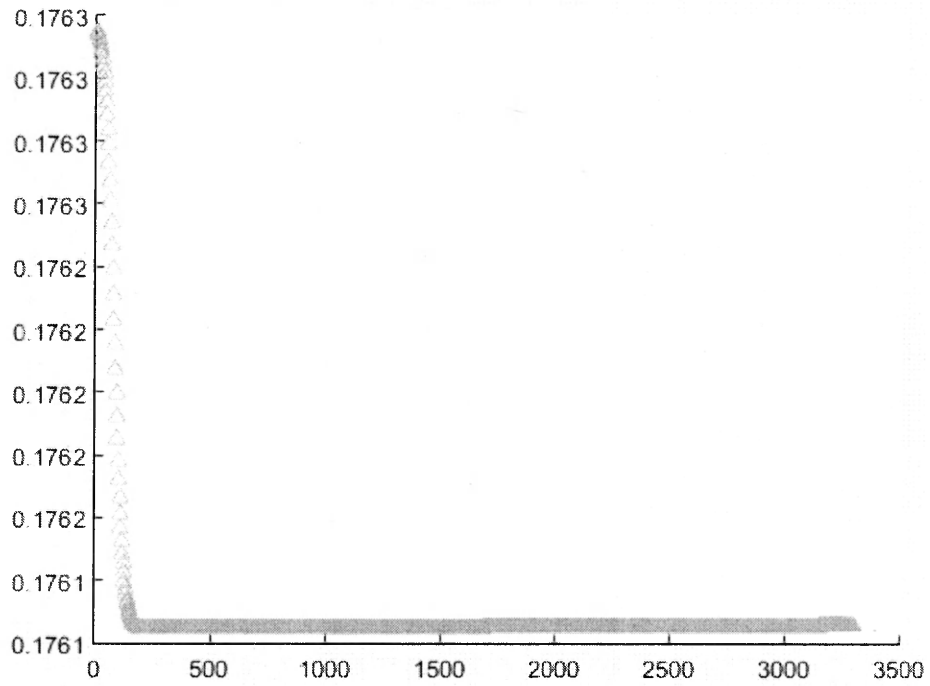
Figure 53: Harmine Concentration Range 200:380 with minimum

X: 287.387387387387
Y: 0.176124126830265
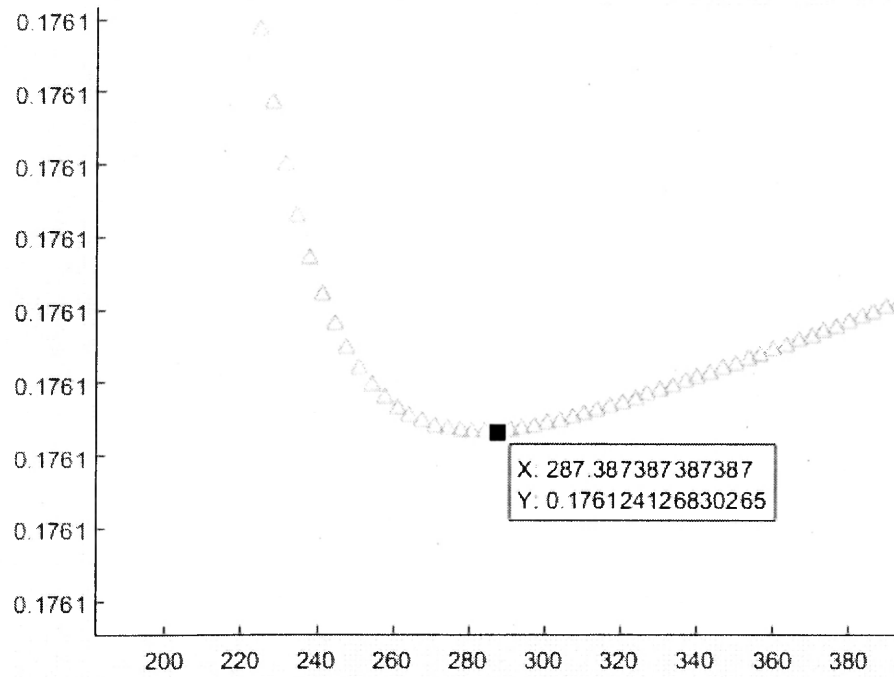
Seleciclib Plots

Figure 54: Seleciclib Concentration Range 0:9000 (~30x IC50)
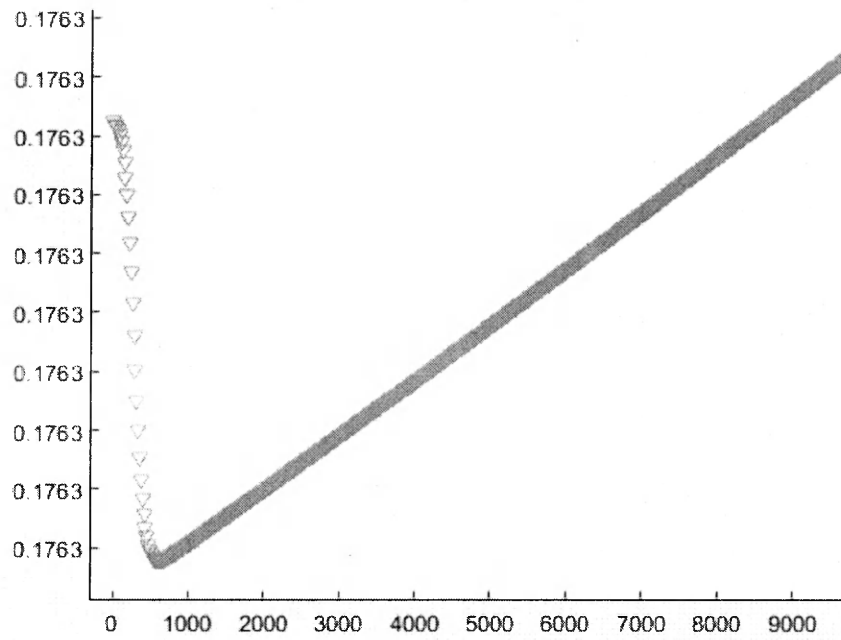
Figure 55: Seleciclib Concentration Range 400:900 with minimum
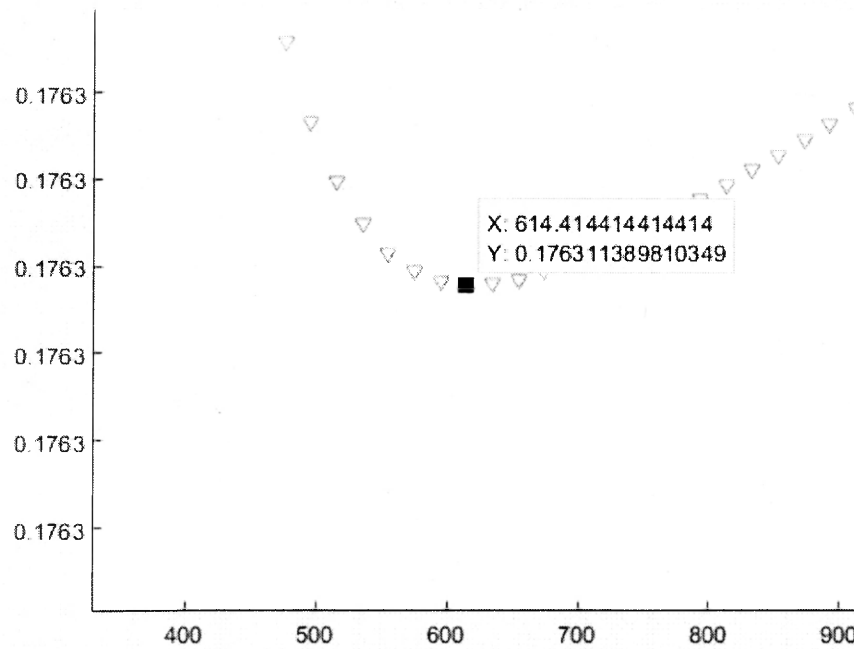
Brysostatin Plot (High Toxicity Plot)

Figure 56: Bryostatin Concentration Range 0:2000
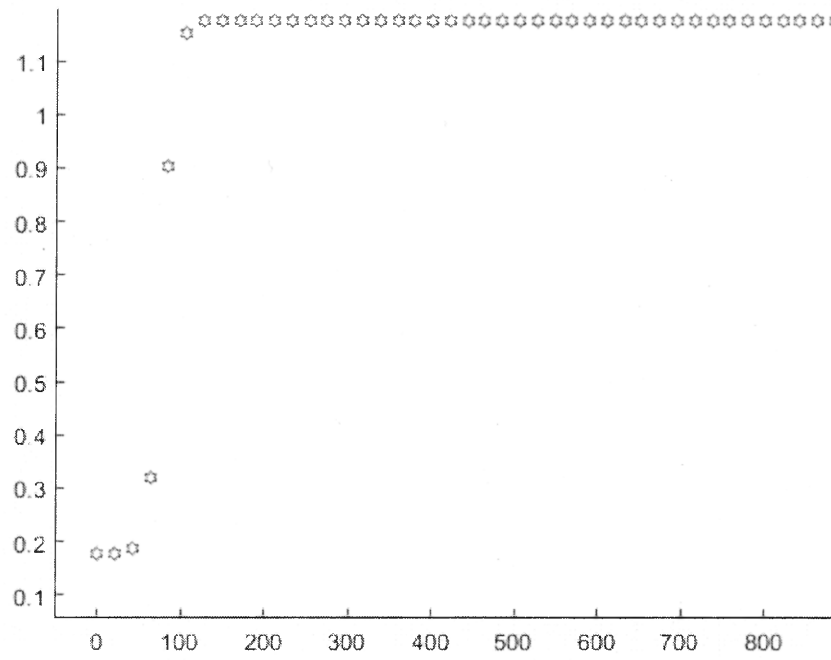
Alpha BTX Plot (Toxin Plot)

Figure 57: Alpha BTX Concentration Range -80:60
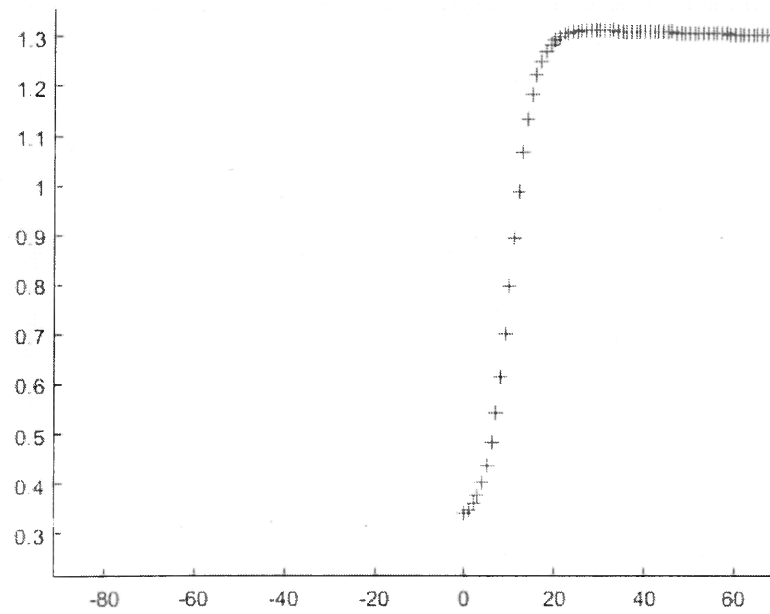
Figure 58: Table of Minima Compared to LD50 Values and Apoptosis Rankings

Molecule of Interest	LD50 (nM)	Minimum (nM)	% Minimum of LD50	Apoptosis Relative Value	Apoptosis Rank Lowest to Highest
SP-600125	2500.00	225.135	9.005	0.1723165	2
(R)-CR8	6960000.00	400.800	0.006	0.1763066	5
6-BIO	9000.00	10.300	0.114	0.1763112	7
AR014418	320910.00	228.820	0.071	0.1763109	6
SB-239063	6921.82	---	---	--	9
Paclitaxel 'Derivative'	38857.71	2769.519	7.127	0.1693046	1
Heparin	211555.00	1870.870	0.884	0.1757427	3
Harmine	1170000.00	287.387	0.025	0.1761241	4
Seleciclib	1010000.00	614.414	0.061	0.1763113	8
Bryostatin	76.64	---	---	---	---
Alpha-BTX	10.22	---	---	---	---

DISCUSSION

Figures 37 and 38 show the theoretical constructed healthy and disease states respectively. Everything is within a few order of magnitudes, which is accurate for resting concentrations of molecules within the cell. The disease state shows the value of hyper tau to be over almost 15x the value of hyper tau in the normal state, at a resounding 15.181818 nM. This is the hyper tau increase which is responsible for the neurofibrillary tangles.

Figures 39 through 57 show the apoptosis versus concentration plots for each drug, starting from relative apoptosis value at approximately 0.176325. This value is a relatively arbitrary value used as a value that seems to make simple sense. All the cells cannot die, but a large portion must die for the memory loss to occur. 0.176325, being between 10 and 20% is a good estimation, seeing that AD brains shrink by approximately that percentage compared to non-diseased patient brains. A tedious algorithm of finding the minimum apoptosis value was enacted via running the code on different concentration ranges at varying resolutions to find the best minimum. After many hours of generating plots using some of the highest resolutions that even a computer with 16 individual core processors can handle, the minima were all located on the drugs which worked and were tabulated in Figure 58.

Figure 58 shows each molecule of interest's determined minimum concentration (X-coordinate) and database LD50 value. It also shows the apoptosis minimum value (Y-coordinate). None of the apoptosis values diminish by a great percentage. Some appear to not shrink at all from the intitial 0.176325 value upon

56

initial inspection. This is because some of our toxicity levels, tau in particular, are set to counter the effects of many drugs in tandem, not individually. This is a great way to discover the drugs which do not work the best, seen by SB-239063 in Figure 47 because it does not even have a value that begins to decrease apoptosis under the computationally imposed toxicity stresses. Thus the drugs do not appear effective numerically until the differences between the values are taken into consideration; everything is relative here. Additionally, rankings are assigned based on the lowest and highest resultant apoptosis values.

The green shaded values under each column represent the best value in that column. In the Minimum column, the green shaded value represents the lowest drug concentration used. The shaded green values under the % Minimum of LD50 column represent the drug effectiveness in that those drugs shaded were effective at reducing apoptosis with very low concentration percentage of their LD50 value.

Paclitaxel is shaded blue because I wanted to implement a random neutral hypothetical molecule into the model. Ignoring its potential therapies as a microtubule stabilizer, if Paclitaxel was an inhibitor instead of an activator, the values generated are reported in Figure 58 The lowest apoptosis value mean that a very similar derivative that functions oppositely to Paclitaxel may prove therapeutic regarding the parameters and considerations of this study. Essentially, this is demonstrating the power of BST modeling and endless hypothetical possibilities that can be incorporated into future work.

Alpha-BTX was incorporated into the model to show that it is indeed a toxin and also to portray what the graph of a toxin would look like compared to the other

drugs, as seen in Figure 57. Similarly, however, bryostatin 1 in Figure 56 shows

reverse activity, despite it being a potent PKC inhibitor. This is due to its very small

LD50 value, a value that is only 10x the LD50 of Alpha-BTX at 77nM. Essentially the

cell dies before the therapeutic effects take place, so it portrays behavior similar to a

true toxin. Alpha-BTX and Bryostatin 1 and accordingly both shaded red in Figure 56,

meaning that they are not therapeutic in the slightest.

The best mathematical solution to the problem of Alzheimer's disease

apoptosis presented by this model and set of system of differential equations is SP-

600125. It simply has the best apoptosis relative value, excluding hypothetical

paclitaxel derivative. Even though its % Minimum of LD50 is the worst relatively, it is

still below 10% of the LD50 value, coming in at 9.005. The second best choice is

Heparin, which has the second best apoptosis relative value excluding hypothetical

paclitaxel derivative, and interestingly enough, has one of the lower % Minimum of

LD50 values.   An alternative, if one is only interested in % of LD50, is Harmine, as it

achieves the third lowest apoptosis relative value excluding hypothetical paclitaxel

derivative while maintaining the lowest % of LD50 concentration required to achieve

said minimum.

CONCLUSION

Using biological systems theory (BST), it has been confirmed that most of these drugs perform their preconceived functions regarding inhibition and activation of tau protein kinases. It has been concluded that SP-600125 is the best mathematical choice for Alzheimer's disease therapy. It has also been concluded that Heparin and Harmine are the alternative situational mathematical choices for Alzheimer's disease therapy. It has additionally been concluded that bryostatin is a pseudo toxin, resembling alpha-BTX in that it is too toxic to portray therapeutic results mathematically. It has also been concluded that SB-239063 is the worst choice for a drug that does not act as a pseudo toxin.

Methods such as those conducted by this research group utilizing BST are providing the essential theoretical information to start cutting edge research projects around the globe in effort to slow the progression if find the elusive cure to this deadly disease, as it can be one of the worst to watch happen. It can occur very early in life relative to the current life expectancies of our era, and last for a long time thereafter, proving challenging for caregivers. Caregiving is the last resort after treatments and other management techniques are applied. In terms of medicated prevention, no medication has been proven statistically, totally effective, resulting in alternative methods, ranging from mentally stimulating activities to ultrasound technology.

VITA

Patrick Neil Blank

Patrick Neil Blank was born in Philadelphia, Pennsylvania on July 26, 1991. He graduated from The Collegiate School of Richmond, Virginia in June of 2010 and went on to study chemistry and mathematics at The College of William and Mary. He earned his B.S. in Chemistry in December of 2013. He continued studying chemistry at The College of William and Mary, and defended his master's thesis on May 8th, 2015. He will begin further studying of chemistry at The University of Pennsylvania in August of 2015. Essentially, he will be returning to his roots.

BIBLIOGRAPHY

References Cited:

(1) Abraham RT1, Acquarone M, Andersen A, Asensi A, Bellé R, Berger F, Bergounioux C, Brunn G, Buquet-Fagot C, Fagot D, et al. (1995). "Cellular effects of olomoucine, an inhibitor of cyclin-dependent kinases" *Biol Cell.* 83(2-3):105-20.

(2) Alzheimer's Disease — History & Description. (2008). Retrieved April 14, 2013, from http://www.best-alzheimers-products.com/alzheimer's-disease.html

(3) Association, A. (n.d.). Seven Stages of Alzheimer's. Retrieved from https://www.alz.org/alzheimers_disease_stages_of_alzheimers.asp

(4) Bahr, B. A. (2003). *Focus on Alzheimer's Disease Research* (E. M. Welsh, Ed.). Nova Biomedical Books.

(5) Borgne A, Meijer L[1], Mulner O, Chong JP, Blow JJ, Inagaki N, Inagaki M, Delcros JG, Moulinoux JP. (1997). "Biochemical and cellular effects of roscovitine, a potent and selective inhibitor of the cyclin-dependent kinases cdc2, cdk2 and cdk5." *Eur J Biochem.*243(1-2):527-36.

(6) Cole, Adam. Soutar, Marc P. M. (2008). "Relative Resistance of Cdk5-phosphorylated CRMP2 to Dephosphorylation." *J Biol Chem.* 283(26): 18227–18237.

(7) Eldar-Finkelman H, Martinez A (2011). "GSK-3 Inhibitors: Preclinical and Clinical Focus on CNS" *Front Mol Neurosci* 32(4).

(8) Embi N, Rylatt DB, Cohen P (June 1980). "Glycogen synthase kinase-3 from rabbit skeletal muscle. Separation from cyclic-AMP-dependent protein kinase and phosphorylase kinase" *Eur J Biochem* 107 (2): 519–27.

(9) Gong, C-X; Iqbal, K. (2008) "Hyperphosphorylation of Microtubule-Associated Protein Tau: A Promising Therapeutic Target for Alzheimer Disease." *Current Medicinal Chemistry* 23(15): 2321-8.

(10) Hirokawa, N. (1988). Tau Proteins: The Molecular Structure and Mode of Binding on Microtubules. *Journal of Cell Biology, 107,* 1449-1459.

(11) Leclerc, Sophie (2000). Indirubins Inhibit Glycogen Synthase Kinase-3β and CDK5/P25, Two Protein Kinases Involved in Abnormal Tau Phosphorylation in Alzheimer's Disease. *The Journal of Biological Chemistry*, 276, 251-260.

(12) Lichtenthaler, S. F. (2010). Alpha-Secretase in Alzheimer's Disease: molecular identity, regulation and therapeutic potential. *Journal of Neurochemistry, 116*(1).

(13) Mandelkow, E. M., & Mandelkow, E. (2012). Biochemistry and Cell Biology of Tau Protein in Neurofibrillary Degeneration. *Cold Spring Harbor Laboratory Press*, 1-25.

(14) Martinez, Ana*; Castro, Ana; Dorronsoro, Isabel. Glycogen Synthase Kinase 3 (GSK-3)Inhibitors as New Promising Drugs for Diabetes,Neurodegeneration, Cancer, and Inflammation.

(15) Meijer1, A-MWH Thunnissen2*, AW White3, M Garnier1, M Nikolic4†,L-H Tsai4, J Walter5, KE Cleverley6, PC Salinas6, Y-Z Wu7, J Biernat7, E-M

Mandelkow7, S-H Kim2 and GR Pettit3. Inhibition of cyclin-dependent kinases, GSK-3b and CK1 by hymenialdisine, a marine sponge constituent.

(16) Michala Kolarova, Francisco García-Sierra, Ales Bartos, Jan Ricny, and Daniela Ripova.(2012) Structure and Pathology of Tau Protein in Alzheimer Disease .*International Journal of Alzheimer's Disease*,1-13.

(17) Pimplikar, S. W., Nixon, R. A., Robakis, N. K., Shen, J., & Tsal, L.-H. (2010). Amyloid-Independent Mechanisms in Alzheimer's Disease Pathogenesis. *The Journal of Neuroscience, 30*(45), 14946-14954.

(18) Sausville, Edward A. (2002) "Complexities in the development of cyclin-dependent kinase inhibitor drugs." *Trends in Molecular Medicine.* 8:S32-S37

(19) Selenica M. L., Jensen H. S., Larsen A. K., Pedersen M. L., Helboe L., Leist M., Lotharius J. (2007). Efficacy of small-molecule glycogen synthase kinase-3 inhibitors in the postnatal rat model of tau hyperphosphorylation. Br. J. Pharmacol. 152, 959–979.10.1038

(20) Tsuji S, Morinobu S, Tanaka K, Kawano K, Yamawaki S. (2003). "Lithium, but not valproate, induces the serine/threonine phosphatase activity of protein phosphatase 2A in the rat brain, without affecting its expression." *J Neural Transm.*110(4):413-25.

(21) Villerbu N1, Gaben AM, Redeuilh G, Mester J. (2002)." Cellular effects of purvalanol A: a specific inhibitor of cyclin-dependent kinase activities. *Int J Cancer.* 97(6):761-9.

(22) Xu Y, Xing Y, Chen Y, Chao Y, Lin Z, Fan E, Yu JW, Strack S, Jeffrey PD, Shi Y. (2006) "Structure of the protein phosphatase 2A holoenzyme." *Cell.* 127(6):1239-51

(23) Yan Xiong, Xiao-Peng Jing, Xin-Wen Zhou, Xiu-Lian Wang, Yang Yang, Xu-Ying Sun, Mei Qiu, Fu-Yuan Cao, You-Ming Lu, Rong Liu, Jian-Zhi Wang, Zinc induces protein phosphatase 2A inactivation and tau hyperphosphorylation through Src dependent PP2A (tyrosine 307) phosphorylation, *Neurobiology of Aging*, Volume 34, Issue 3, March 2013, Pages 745-756, ISSN 0197-4580

(24) Yvette Mettey,†, Marie Gompel,‡, Virginie Thomas,‡, Matthieu Garnier,‡, Maryse Leost,‡, Irène Ceballos-Picot,§, Martin Noble,⊥, Jane Endicott,⊥, Jean-michel Vierfond,† and, and Laurent Meijer*,‡ (2003). "Aloisines, a New Family of CDK/GSK-3 Inhibitors. SAR Study, Crystal Structure in Complex with CDK2, Enzyme Selectivity, and Cellular Effects."*Journal of Medicinal Chemistry.* 46(2), 222-236